Conservative Semi-LAgrangian Multi-tracer scheme (CSLAM): a semi-implicit shallow water and a fully compressible non-hydrostatic solver with fully consistent transport

Peter Hjort Lauritzen

Atmospheric Modeling & Predictability Section
Climate & Global Dynamics Division
National Center for Atmospheric Research (NCAR), Boulder, Colorado

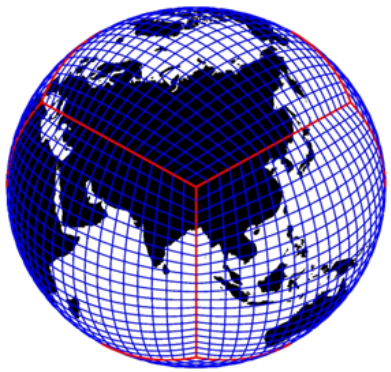
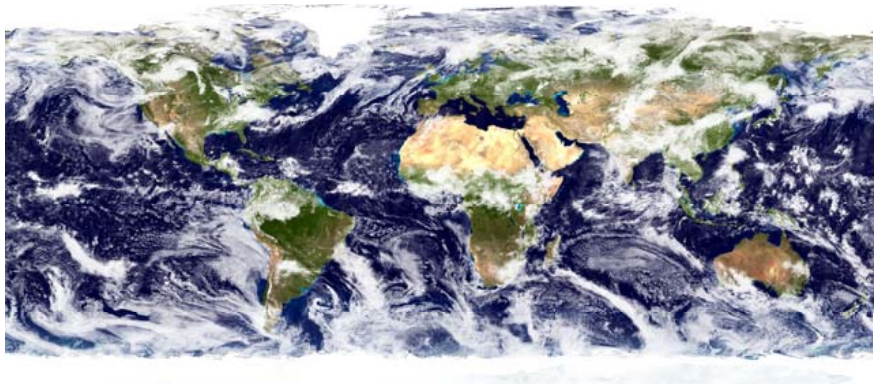


Collaborators: M. Wong (University of British Columbia, Vancouver), W.C. Skamarock (NCAR), R.D. Nair (NCAR), J. Thuburn (University of Exeter), L. Harris (Geophysical Fluid Dynamics Laboratory, Princeton), P.A. Ullrich (University of California at Davis), C. Erath (Colorado University)

1. CSLAM transport scheme
   - formulation
   - air-tracer mass coupling
   - conditions for local mass-conservation
   - extension to there sphere: gnomonic coordinates
   - CSLAM in NCAR's CAM-SE (Community Atmosphere Model - Spectral Element)

2. CSLAM-SW: shallow water model
   - semi-implicit time-stepping of tracers
   - treatment of divergence

3. CSLAM-NH: non-hydrostatic $x - z$ plane solver
   - preliminary results

Design (see fuller discussion in Lauritzen et al., 2011)

- Multi-tracer efficiency

  → CAM5 has 31 continuity equations
  (micro-physics and convection scheme developers are eager to add more!)

  → CAM-Chem has approximately 107 continuity equations
- Shape-preservation (large gradients, physics)
- Consistency (air $\leftrightarrow$ tracer)
- Correlation accuracy
- Efficiency on 'traditional[1]' massively parallel machines:
  - *minimize frequency of message passing*: e.g. long Δt's (semi-Lagrangian)
  - *minimize message sizes*: local computational stencil
  - *minimize memory usage*: e.g., 2-time-level, no multi-moment
- Accuracy on non-orthogonal grids (splitting errors) $\Rightarrow$ fully two-dimensional methods

[1] GPUs and Intel MIC architectures??

Design (see fuller discussion in Lauritzen et al., 2011)

- Multi-tracer efficiency
- Shape-preservation (large gradients, physics)

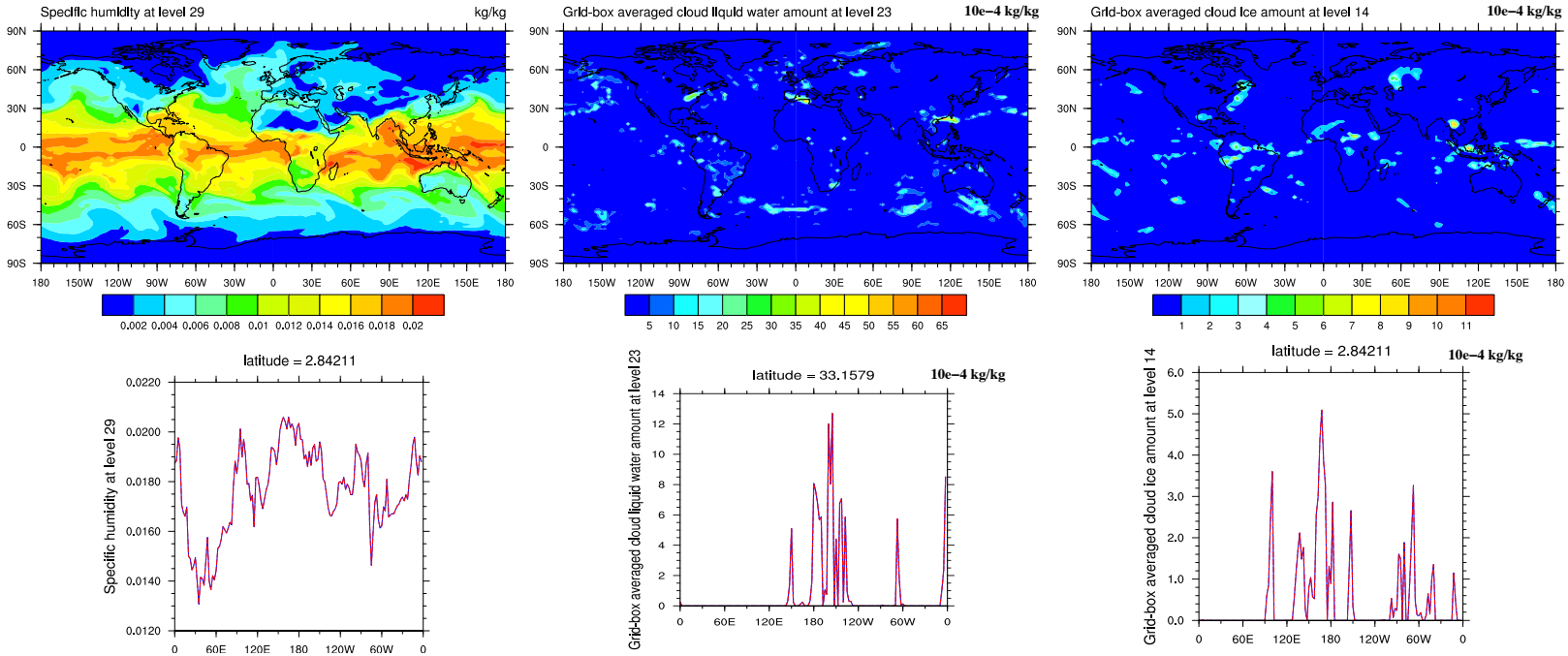

- Consistency (air $\leftrightarrow$ tracer)
- Correlation accuracy
- Efficiency on 'traditional[1]' massively parallel machines:
  - *minimize frequency of message passing*: e.g. long Δt's (semi-Lagrangian)
  - *minimize message sizes*: local computational stencil
  - *minimize memory usage*: e.g. 2-time-level, no multi-moment

Design (see fuller discussion in Lauritzen et al., 2011)

- Multi-tracer efficiency
- Shape-preservation (large gradients, physics)
- Consistency (air $\leftrightarrow$ tracer)

Consider flux-form continuity equations for air mass and tracer mass:

$$\frac{\partial \rho}{\partial t} + \nabla \cdot (\rho \, \vec{v}) = 0, \tag{1}$$

$$\frac{\partial (\rho \, q)}{\partial t} + \nabla \cdot (\rho q \, \vec{v}) = 0, \tag{2}$$

where ρ is air density and q is tracer mixing ratio. 'Free-stream' preservation implies that the discretization scheme for (2) reduces to (1) when $q = 1$.

- Correlation accuracy
- Efficiency on 'traditional[1]' massively parallel machines:
  - *minimize frequency of message passing*: e.g. long Δt's (semi-Lagrangian)
  - *minimize message sizes*: local computational stencil
  - *minimize memory usage*: e.g., 2-time-level, no multi-moment
- Accuracy on non-orthogonal grids (splitting errors) $\Rightarrow$ fully two-dimensional methods

[1] GPUs and Intel MIC architectures??

Design (see fuller discussion in Lauritzen et al., 2011)

- Multi-tracer efficiency
- Shape-preservation (large gradients, physics)
- Consistency (air $\leftrightarrow$ tracer)
- Correlation accuracy

Relationships between long-lived stratospheric tracers, manifested in similar spatial structures on scales ranging from a few to several thousand kilometers, are displayed most strikingly if the mixing ratio of one is plotted against another, when the data collapse onto remarkably compact curves. - Plumb (2007)

E.g., when plotting nitrous oxide (N_2O) against 'total odd nitrogen' (NO_y) or chlorofluorocarbon (CFC's)

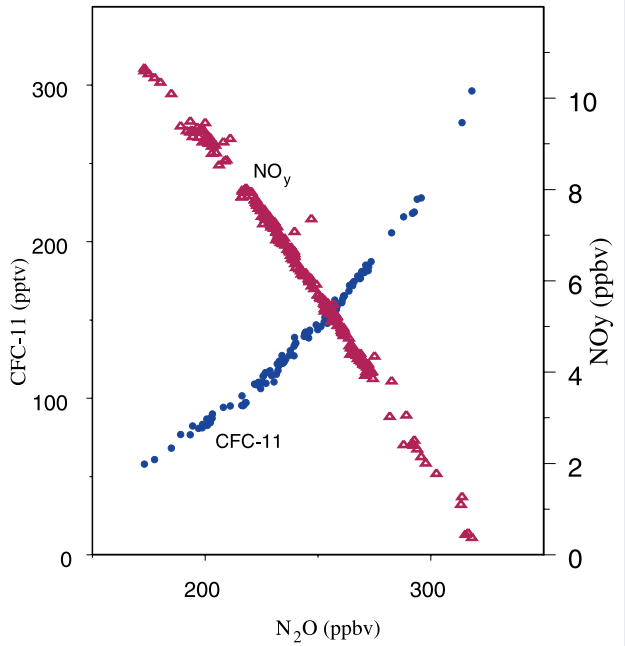

It is therefore highly desirable that the transport schemes used in chemistry and chemistry-climate models should not disrupt such functional relations in unphysical ways through numerical mixing or, indeed, unmixing.' -(Lauritzen and Thuburn, 2012)

Design (see fuller discussion in Lauritzen et al., 2011)

- Multi-tracer efficiency
- Shape-preservation (large gradients, physics)
- Consistency (air $\leftrightarrow$ tracer)
- Correlation accuracy
- Efficiency on 'traditional[1]' massively parallel machines:
  - *minimize frequency of message passing*: e.g. long Δt's (semi-Lagrangian)
  - *minimize message sizes*: local computational stencil
  - *minimize memory usage*: e.g., 2-time-level, no multi-moment

NCAR's Yellowstone is a 1.5-petaflops high-performance computing system with 72,288 processor cores.

- Accuracy on non-orthogonal grids (splitting errors) $\Rightarrow$ fully two-dimensional methods

[1] GPUs and Intel MIC architectures??

Design (see fuller discussion in Lauritzen et al., 2011)

- Multi-tracer efficiency
- Shape-preservation (large gradients, physics)
- Consistency (air $\leftrightarrow$ tracer)
- Correlation accuracy
- Efficiency on 'traditional[1]' massively parallel machines:
  - *minimize frequency of message passing*: e.g. long Δt's (semi-Lagrangian)
  - *minimize message sizes*: local computational stencil
  - *minimize memory usage*: e.g., 2-time-level, no multi-moment

NCAR's Yellowstone is a 1.5-petaflops high-performance computing system with 72,288 processor cores.

- Accuracy on non-orthogonal grids (splitting errors) $\Rightarrow$ fully two-dimensional methods

[1] GPUs and Intel MIC architectures??

Design (see fuller discussion in Lauritzen et al., 2011)

- Multi-tracer efficiency
- Shape-preservation (large gradients, physics)
- Consistency (air $\leftrightarrow$ tracer)
- Correlation accuracy
- Efficiency on 'traditional[1]' massively parallel machines:
  - *minimize frequency of message passing*: e.g. long Δt's (semi-Lagrangian)
  - *minimize message sizes*: local computational stencil
  - *minimize memory usage*: e.g., 2-time-level, no multi-moment

NCAR's Yellowstone is a 1.5-petaflops high-performance computing system with 72,288 processor cores.

- Accuracy on non-orthogonal grids (splitting errors) $\Rightarrow$ fully two-dimensional methods

[1] GPUs and Intel MIC architectures??

Design (see fuller discussion in Lauritzen et al., 2011)

- Multi-tracer efficiency
- Shape-preservation (large gradients, physics)
- Consistency (air $\leftrightarrow$ tracer)
- Correlation accuracy
- Efficiency on 'traditional[1]' massively parallel machines:
  - *minimize frequency of message passing*: e.g. long Δt's (semi-Lagrangian)
  - *minimize message sizes*: local computational stencil
  - *minimize memory usage*: e.g., 2-time-level, no multi-moment

NCAR's Yellowstone is a 1.5-petaflops high-performance computing system with 72,288 processor cores.

- Accuracy on non-orthogonal grids (splitting errors) $\Rightarrow$ fully two-dimensional methods

[1] GPUs and Intel MIC architectures??

Design (see fuller discussion in Lauritzen et al., 2011)

- Multi-tracer efficiency
- Shape-preservation (large gradients, physics)
- Consistency (air $\leftrightarrow$ tracer)
- Correlation accuracy
- Efficiency on 'traditional[1]' massively parallel machines:
  - *minimize frequency of message passing*: e.g. long Δt's (semi-Lagrangian)
  - *minimize message sizes*: local computational stencil
  - *minimize memory usage*: e.g., 2-time-level, no multi-moment
- Accuracy on non-orthogonal grids (splitting errors) $\Rightarrow$ fully two-dimensional methods

reg. lat-lon

cubed-sphere

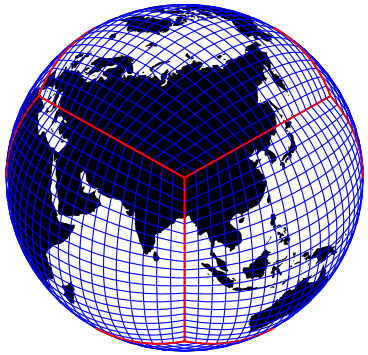

Voronoi

Yin-Yang

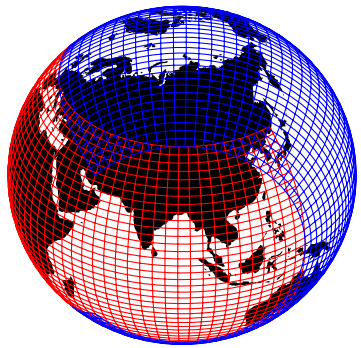

[1] GPUs and Intel MIC architectures??

Part I
New geometrically flexible multi-tracer scheme

Conservative Semi-LAgrangian Multi-tracer (CSLAM); Lauritzen et al. (2010)

CSLAM is based on pioneering work by Dukowicz (1984), Ramshaw (1985), Dukowicz and Baumgardner (2000), and Margolin and Shashkov (2003)!

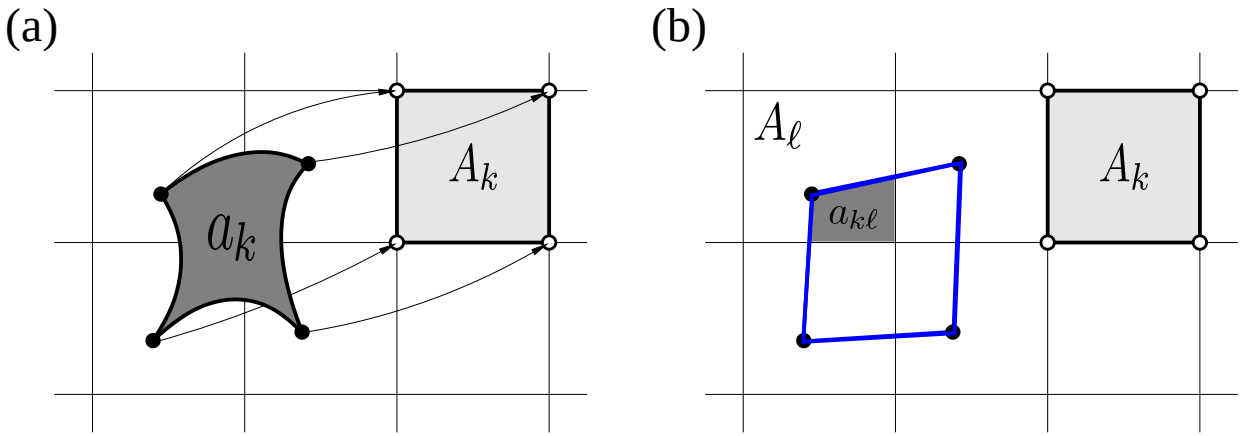

Finite-volume Lagrangian form of continuity equation for $\psi = \rho, \rho\,\phi$:

$$\int_{A_k} \psi_k^{n+1}\, dx\, dy = \int_{a_k} \psi_k^{n}\, dx\, dy \quad = \quad \sum_{\ell=1}^{L_k} \iint_{a_{k\ell}} f_\ell(x,y)\, dx\, dy,$$

where the $a_{k\ell}$'s are non-empty overlap regions:

$$a_{k\ell} = a_k \cap A_\ell, \quad a_{k\ell} \neq \emptyset; \quad \ell = 1, \ldots, L_k. \tag{1}$$

For higher-order upstream cell-edge approximations see Ullrich et al. (2013).

Conservative Semi-LAgrangian Multi-tracer (CSLAM); Lauritzen et al. (2010)

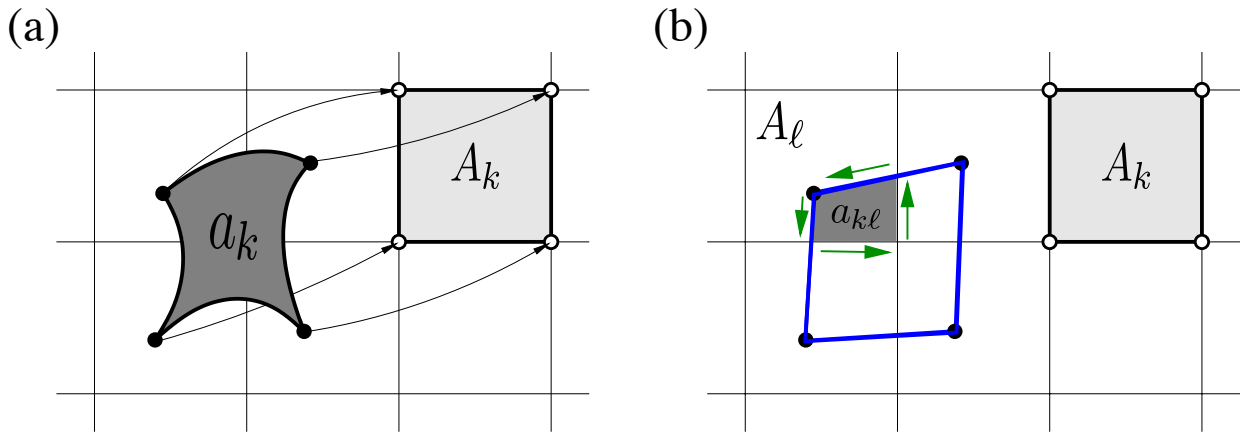

Finite-volume Lagrangian form of continuity equation for $\psi = \rho, \rho\,\phi$:

$$\int_{A_k} \psi_k^{n+1}\,dx\,dy = \int_{a_k} \psi_k^{n}\,dx\,dy \quad = \quad \sum_{\ell=1}^{L_k} \iint_{a_{k\ell}} f_\ell(x,y)\,dx\,dy,$$

where $\partial a_{k\ell}$ is the boundary of $a_{k\ell}$ and

$$f_\ell(x,y) = \sum_{i+j\le 2} c_\ell^{(i,j)} x^i y^j.$$

Conservative Semi-LAgrangian Multi-tracer (CSLAM); Lauritzen et al. (2010)

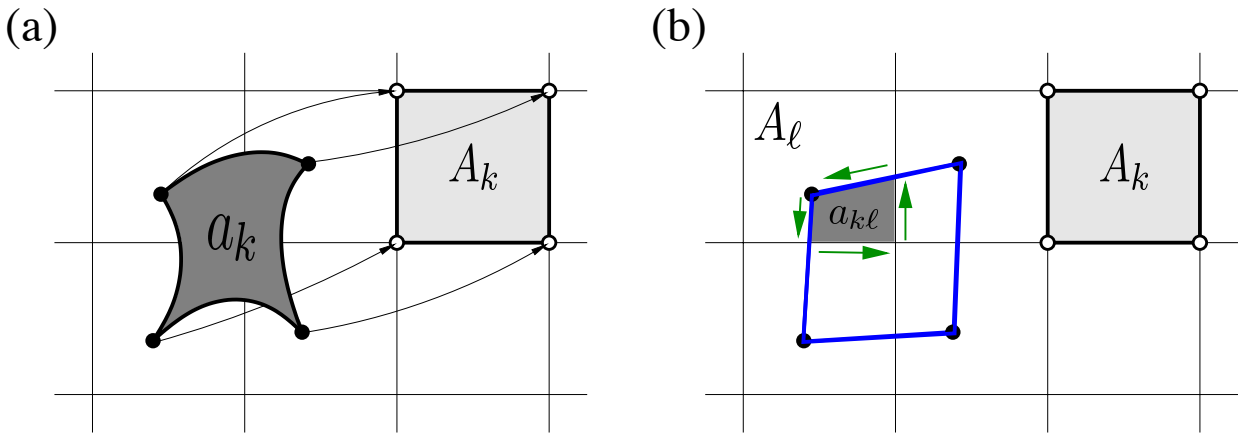

Finite-volume Lagrangian form of continuity equation for $\psi = \rho, \rho\,\phi$:

$$\int_{A_k} \psi_k^{n+1}\, dx\, dy = \int_{a_k} \psi_k^{n}\, dx\, dy \quad = \quad \sum_{\ell=1}^{L_k} \oint_{\partial a_{k\ell}} \left[P\, dx + Q\, dy\right],$$

where $\partial a_{k\ell}$ is the boundary of $a_{k\ell}$ and

$$\sum_{i+j\leq 2} \left[-\frac{\partial P^{(i,j)}}{\partial y} + \frac{\partial Q^{(i,j)}}{\partial x}\right] = f_\ell(x,y) = \sum_{i+j\leq 2} c_\ell^{(i,j)} x^i y^j.$$

Conservative Semi-LAgrangian Multi-tracer (CSLAM); Lauritzen et al. (2010)

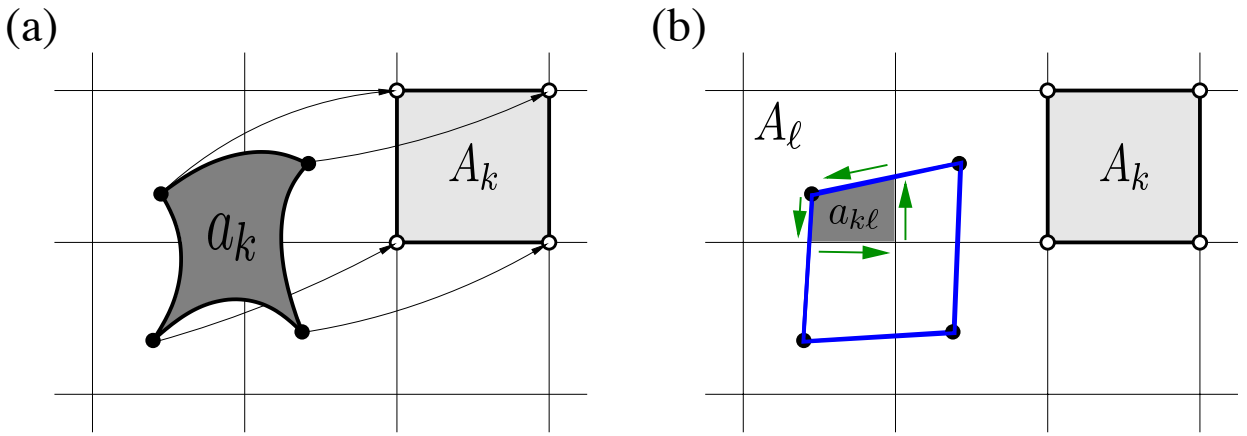

Finite-volume Lagrangian form of continuity equation for $\psi = \rho, \rho\,\phi$:

$$\int_{A_k} \psi_k^{n+1}\,dx\,dy = \int_{a_k} \psi_k^{n}\,dx\,dy \quad = \quad \sum_{\ell=1}^{L_k} \left[\sum_{i+j\leq 2} c_\ell^{(i,j)} w_{k\ell}^{(i,j)} \right],$$

where weights $w_{k\ell}^{(i,j)}$ are functions of the coordinates of the vertices of $a_{k\ell}$.

$w_{k\ell}^{(i,j)}$ can be re-used for each additional tracer $\Rightarrow$ *multi-tracer effciency!*

Air-tracer coupling with cell-integrated Lagrangian schemes

Air density ρ and tracer mixing ratio q must be coupled carefully to ensure:

- mass-conservation
- shape-preservation (q is invariant following parcels; not $\rho\, q$)
- 'free-stream' preservation

A 'Lagrangian' solution (Appendix B of Nair and Lauritzen, 2010)

- In cell k reconstruct sub-grid-scale distribution for ρ and q separately:

$$\rho(x,y) = \sum_{i+j\leq 2} \rho^{(i,j)} x^i y^j \quad \text{and} \quad q(x,y) = \sum_{i+j\leq 2} q^{(i,j)} x^i y^j .$$

- Apply shape-preserving reconstruction filter to $q(x,y)$ (see next slide)
- In Eulerian cell k tracer mass sub-grid-scale reconstruction is:

$$\rho q(x,y) = \overline{\rho}_k\, q_k(x,y) + \overline{q}_k\, \left[\rho_k(x,y) - \overline{\rho}_k\right], \tag{1}$$

where $\overline{(\cdot)}$ is cell average value; $\overline{q}_k = \overline{\rho\, q}_k / \overline{\rho}_k$

$\Rightarrow q = 1 \Rightarrow$ reconstruction (1) reduces to reconstruction of air density!
$\Rightarrow \rho q(x,y)$ is degree 2 (with $\rho q(x,y) = \rho(x,y) \times q(x,y)$ it would have been 4)

Fully 2D reconstruction filter/limiter (Barth and Jespersen, 1989)

Scale the reconstruction function $\psi(x, y)$ so that extreme values lie within the adjacent cell-average values (can be applied selectively for less diffusion, Harris et al., 2010)

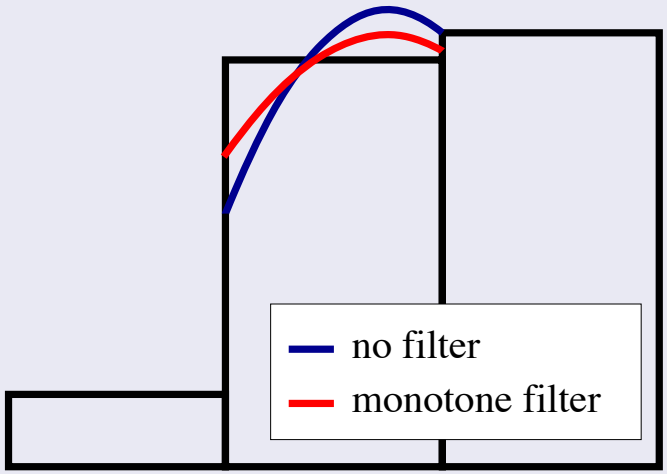

Figure: One-dimensional illustration of fully two-dimensional filter

Note that enforcing shape-preservation is 'harder/stricter' than for flux-form schemes:

- For Lagrangian schemes we can't mix low and high-order fluxes (e.g. Zalesak, 1979)
- Reconstruction functions must satisfy mass-conservation constraint:

$$\int_{A_k} \psi_k(x, y)\, dA = \overline{\psi}_k\, \Delta A_k,$$

where $\overline{\psi}_k$ is cell average value over A_k with area ΔA_k. (more on this in a moment)

Conditions for local mass-conservation (Erath et al., 2013)

- Line-integrals must span the domain without 'cracks/overlaps':

$$\sum_{i \in \mathcal{E}} \Delta a_{ik} = \Delta A_k \quad \text{where} \quad \mathcal{E}_k = \{\ell \,|\, a_{\ell k} \cap A_k \neq \emptyset\} = \{(a, b, c, d, e)\} \tag{2}$$

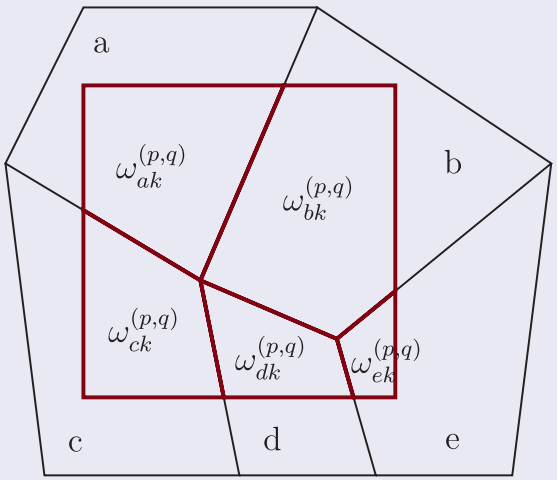

- 'Interior' line-integrals cancel.
- Line-integrals along boundary of Eulerian cell do not cancel since the reconstruction function is not continuous across cell boundaries.

- **Boundary line-integrals must integrate $f_\ell(x, y)$ exactly!**:

$$\sum_{\ell \in \mathcal{E}_k} \left[\sum_{i+j \leq 2} c_\ell^{(i,j)} x^i y^j \right] = \overline{\psi}_k \Delta A_k, \tag{3}$$

Satisfying (3) on sphere can be tricky - next slide!

Line-integrals on the sphere: gnomonic projection

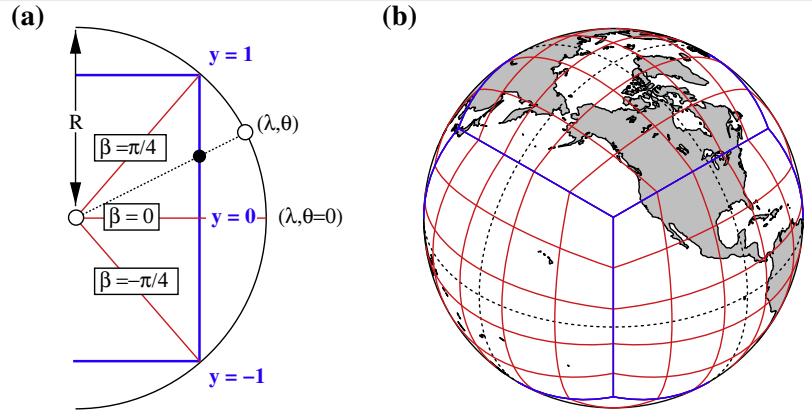

'Cartesian-like' coordinates:

$$(x, y) = R\ (\tan\alpha, \tan\beta) \qquad (4)$$

where R radius and $\alpha, \beta = \left[-\frac{\pi}{4}, \frac{\pi}{4}\right]$ central angles.

Line-integrals for β constant can be computed exactly (Ullrich et al., 2009):
(note: mass-conservation relies on this!)

$$I^{(0,0)} = -\arctan\left(\frac{x\,y}{\rho}\right), \qquad I^{(2,0)} = -y\,\mathrm{arcsinh}\left(\frac{x}{\sqrt{1+y^2}}\right) - \arccos\left(\frac{x}{\sqrt{1+x^2}}\,\frac{y}{\sqrt{1+y^2}}\right),$$

$$I^{(1,0)} = \mathrm{arcsinh}\left(\frac{y}{\sqrt{1+x^2}}\right), \qquad I^{(0,2)} = -x\,\mathrm{arcsinh}\left(\frac{y}{\sqrt{1+x^2}}\right) - \arccos\left(\frac{x}{\sqrt{1+x^2}}\,\frac{y}{\sqrt{1+y^2}}\right),$$

$$I^{(0,1)} = \mathrm{arcsinh}\left(\frac{x}{\sqrt{1+y^2}}\right), \qquad I^{(1,1)} = \rho,$$

$\rightarrow$ some integrals 'ill-conditioned', in particular, at high resolution!

Line-integrals on the sphere: gnomonic projection

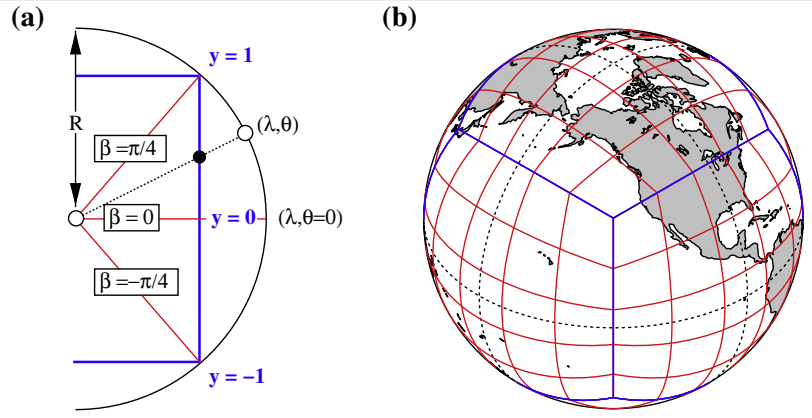

'Cartesian-like' coordinates:

$$(x, y) = R\,(\tan\alpha, \tan\beta) \qquad (4)$$

where R radius and $\alpha, \beta = \left[-\frac{\pi}{4}, \frac{\pi}{4}\right]$ central angles.

Performing line-integrals along cell boundaries with Gaussian quadrature is much more robust, however, integrals are not exact!

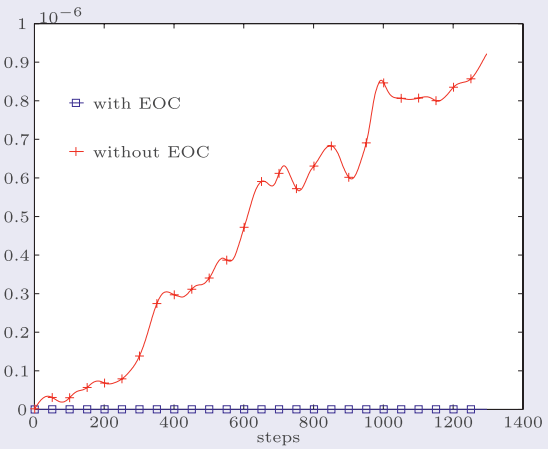

(a) Two Gaussian points for line integrals.

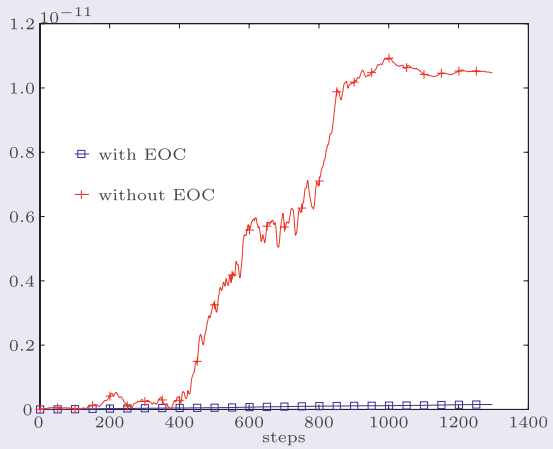

(b) Four Gaussian points for line integrals.

Enforce consistency: Locally scale weights so that

$$\sum_{i\in\mathcal{E}} a_{ik} = A_k \qquad (5)$$

and similarly for higher-order moments.
(Erath et al., 2013)

Accuracy of linear transport (Lauritzen et al., 2012)

New diagnostics/test case suite designed to assess:

1. numerical order of convergence,
2. 'minimal' resolution,
3. ability of the transport scheme to preserve filaments,
4. ability of the transport scheme to transport 'rough' distributions,
5. ability of the transport scheme to preserve pre-existing functional relations between tracers,
6. ability of transport scheme to deal with divergent flows (Nair and Lauritzen, 2010).

Manuscript comparing 17 state-of-the-art schemes using new standard test case suite is almost complete (Lauritzen et al., 2013)

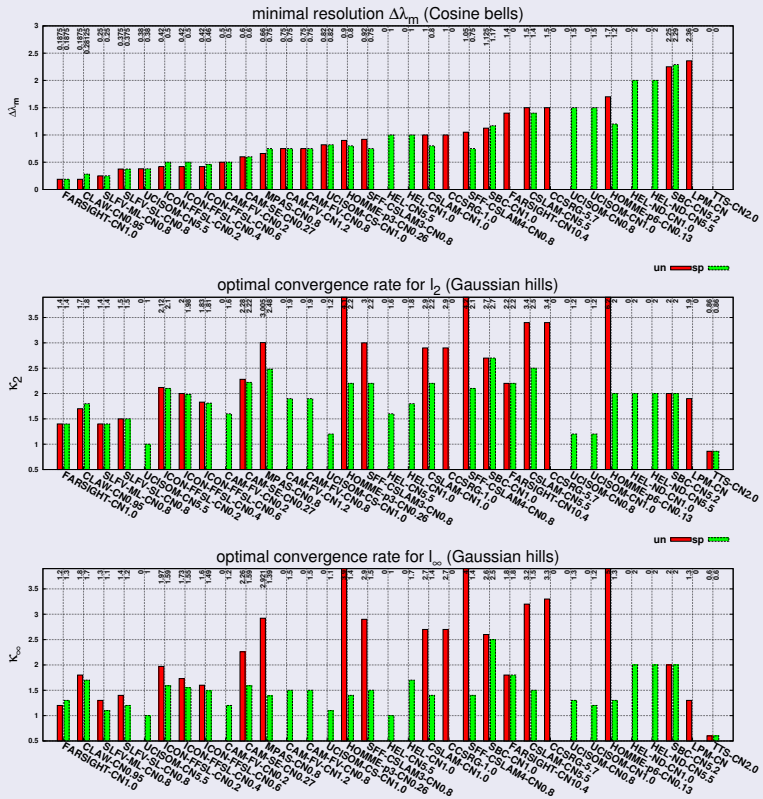

CSLAM implemented in CAM-SE for *'offline'* transport (Erath et al., 2012)

- SE = spectral element dynamical core in CAM/HOMME (Dennis et al., 2012)
- SE uses elements and each element has a quadrature grid
- CSLAM uses an equi-angular gnonomic finite-volume grid

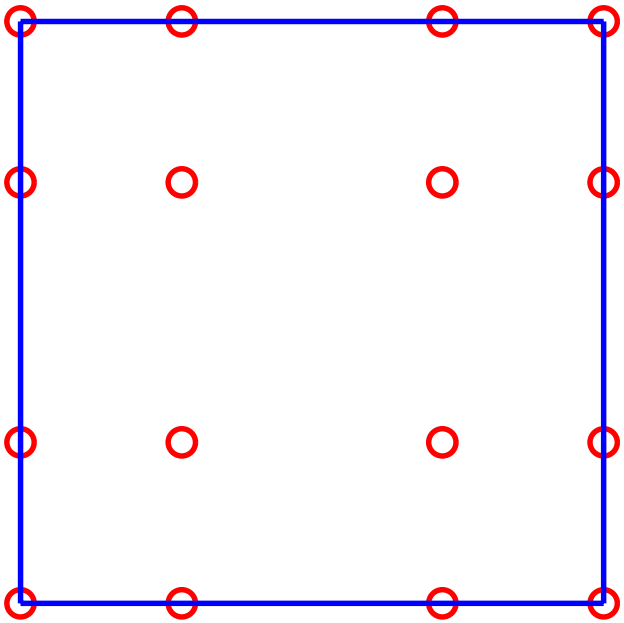

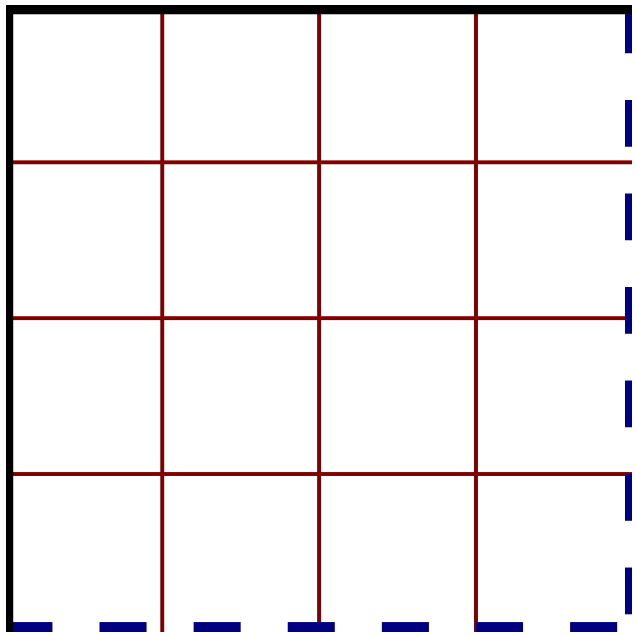

- Figure: (left) 'CSLAM grid' and (right) spectral element quadrature grid
- Infracstructure is being implemented to support coarser or finer finite-volume physics grid (physics grid may, of course, also simply coincide with CSLAM grid).

CSLAM implemented in CAM-SE for *'offline'* transport (Erath et al., 2012)

- SE = spectral element dynamical core in CAM/HOMME (Dennis et al., 2012)
- SE max. Courant number (CN): $CN < 0.28$
- CSLAM max. Courant number for SE implementation: $CN < 1$

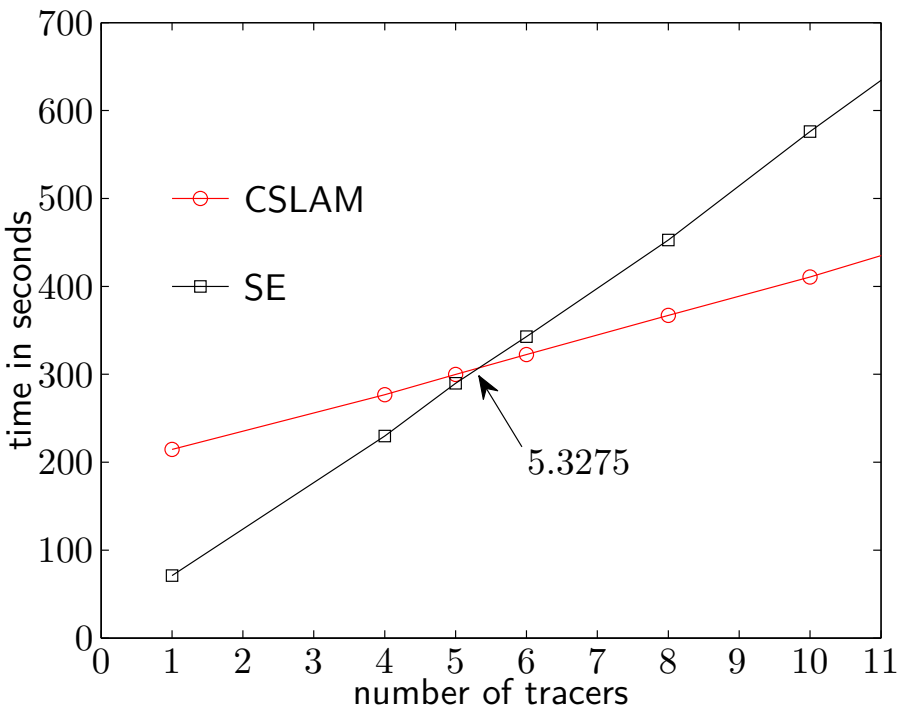

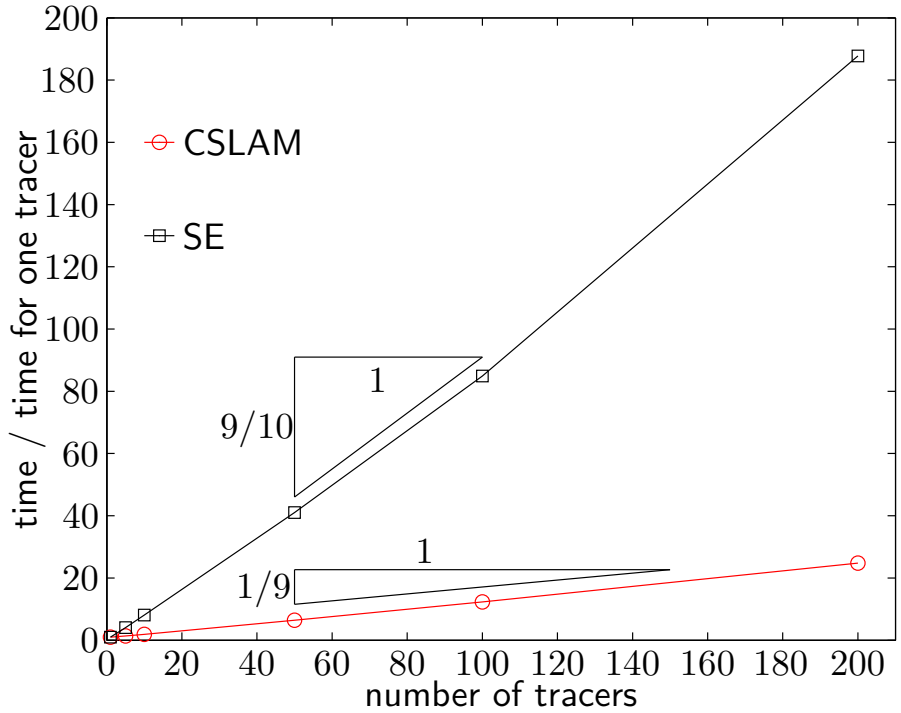

NCAR's Cray XT5m

These performance numbers are for exact trajectories!

'Online' coupling CAM-SE with CSLAM - ongoing work!

Constraints: mass-conservation, consistency, shape-preservation

CAM-SE predicted ρ_{SE} does, obviously, not match 'offline' ρ_{CSLAM} computed by CSLAM!

Possible solutions:

- overwrite ρ_{SE} with ρ_{CSLAM}; unstable?
- nudge ρ_{SE} towards ρ_{CSLAM}; unstable?
- switch to flux-form version of CSLAM (Harris et al., 2010) and use well-known finite-volume method for coupling: SE provides accumulated background flux of air mass and CSLAM provides average flux of q (satisfies all constraints!):

$$\text{Tracer mass flux } =< q >_{CSLAM} \sum_{j=1}^{nsplit} \rho_{SE}^{(n+j/nsplit)}$$

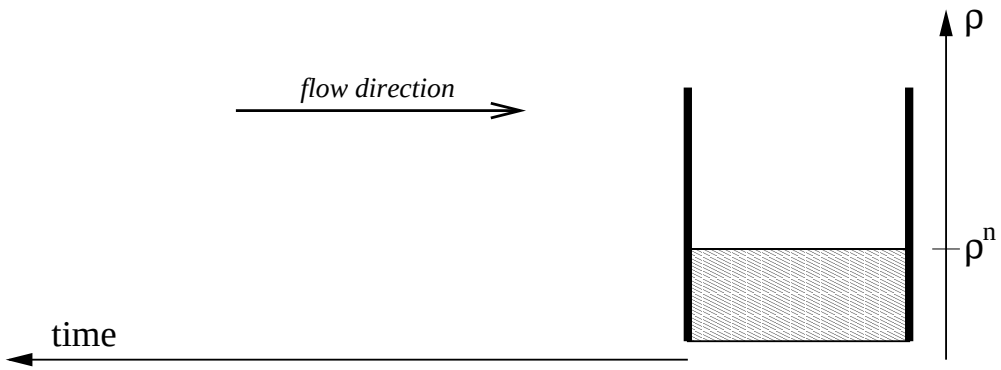

'Online' coupling CAM-SE with CSLAM - ongoing work!

Constraints: mass-conservation, consistency, shape-preservation

CAM-SE predicted ρ_{SE} does, obviously, not match 'offline' ρ_{CSLAM} computed by CSLAM!

Possible solutions:

- overwrite ρ_{SE} with ρ_{CSLAM}; unstable?
- nudge ρ_{SE} towards ρ_{CSLAM}; unstable?
- switch to flux-form version of CSLAM (Harris et al., 2010) and use well-known finite-volume method for coupling: SE provides accumulated background flux of air mass and CSLAM provides average flux of q (satisfies all constraints!):

$$\text{Tracer mass flux } =< q >_{CSLAM} \sum_{j=1}^{nsplit} \rho_{SE}^{(n+j/nsplit)}$$

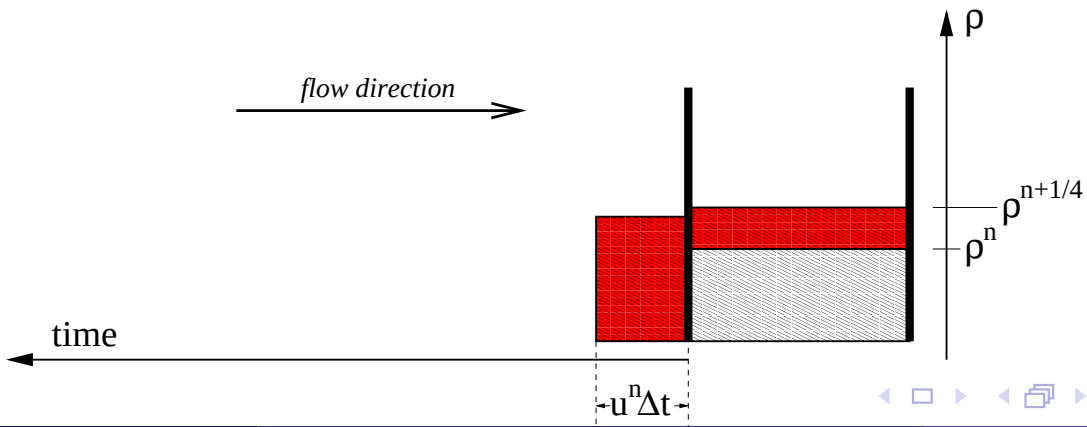

'Online' coupling CAM-SE with CSLAM - ongoing work!

Constraints: mass-conservation, consistency, shape-preservation

CAM-SE predicted ρ_{SE} does, obviously, not match 'offline' ρ_{CSLAM} computed by CSLAM!

Possible solutions:

- overwrite ρ_{SE} with ρ_{CSLAM}; unstable?
- nudge ρ_{SE} towards ρ_{CSLAM}; unstable?
- switch to flux-form version of CSLAM (Harris et al., 2010) and use well-known finite-volume method for coupling: SE provides accumulated background flux of air mass and CSLAM provides average flux of q (satisfies all constraints!):

$$\text{Tracer mass flux } =< q >_{CSLAM} \sum_{j=1}^{nsplit} \rho_{SE}^{(n+j/nsplit)}$$

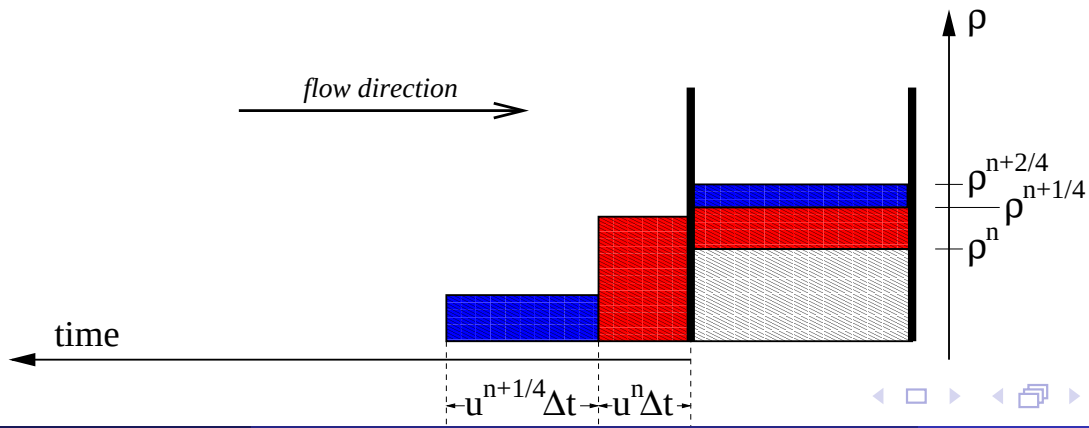

'Online' coupling CAM-SE with CSLAM - ongoing work!

Constraints: mass-conservation, consistency, shape-preservation

CAM-SE predicted ρ_{SE} does, obviously, not match 'offline' ρ_{CSLAM} computed by CSLAM!

Possible solutions:

- overwrite ρ_{SE} with ρ_{CSLAM}; unstable?
- nudge ρ_{SE} towards ρ_{CSLAM}; unstable?
- switch to flux-form version of CSLAM (Harris et al., 2010) and use well-known finite-volume method for coupling: SE provides accumulated background flux of air mass and CSLAM provides average flux of q (satisfies all constraints!):

$$\text{Tracer mass flux } =< q >_{CSLAM} \sum_{j=1}^{nsplit} \rho_{SE}^{(n+j/nsplit)}$$

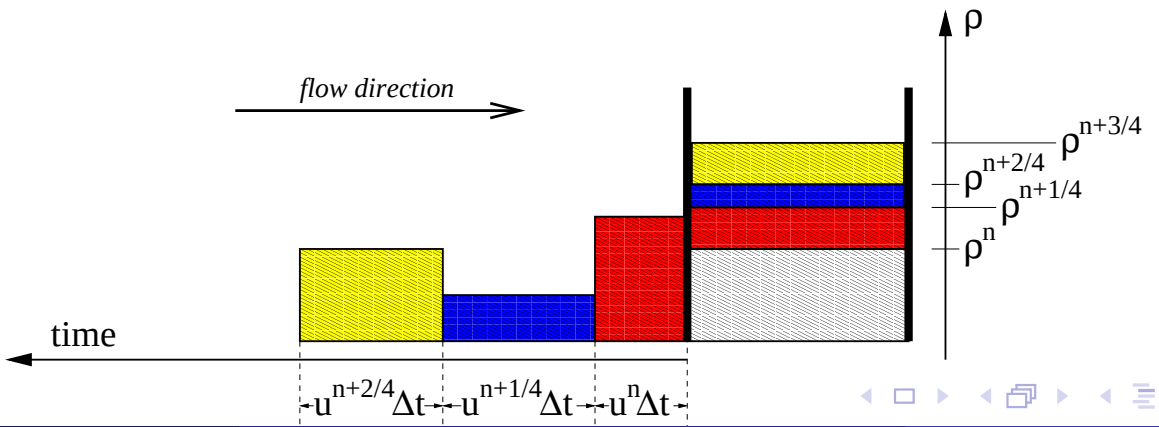

'Online' coupling CAM-SE with CSLAM - ongoing work!

Constraints: mass-conservation, consistency, shape-preservation

CAM-SE predicted ρ_{SE} does, obviously, not match 'offline' ρ_{CSLAM} computed by CSLAM!

Possible solutions:

- overwrite ρ_{SE} with ρ_{CSLAM}; unstable?
- nudge ρ_{SE} towards ρ_{CSLAM}; unstable?
- switch to flux-form version of CSLAM (Harris et al., 2010) and use well-known finite-volume method for coupling: SE provides accumulated background flux of air mass and CSLAM provides average flux of q (satisfies all constraints!):

$$\text{Tracer mass flux } =< q >_{CSLAM} \sum_{j=1}^{nsplit} \rho_{SE}^{(n+j/nsplit)}$$

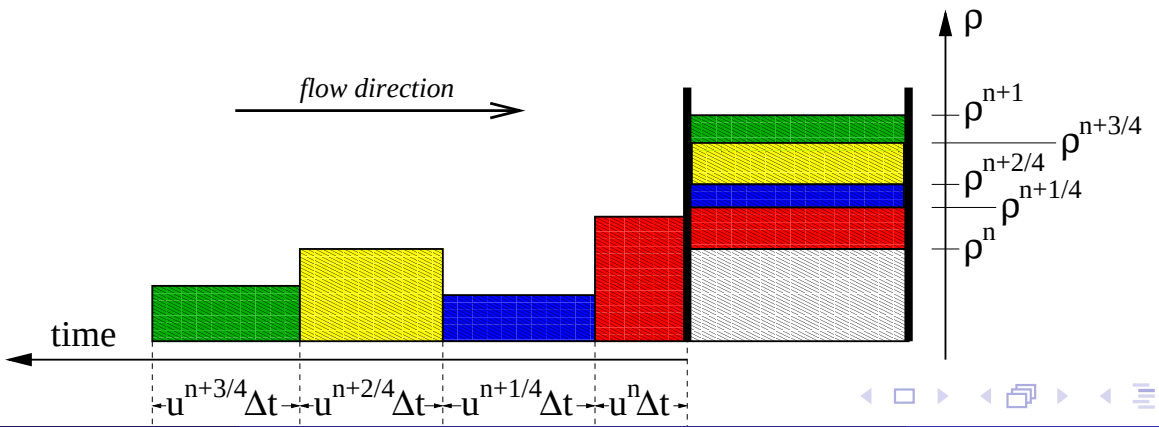

'Online' coupling CAM-SE with CSLAM - ongoing work!

Constraints: mass-conservation, consistency, shape-preservation

CAM-SE predicted ρ_{SE} does, obviously, not match 'offline' ρ_{CSLAM} computed by CSLAM!

Possible solutions:

- overwrite ρ_{SE} with ρ_{CSLAM}; unstable?
- nudge ρ_{SE} towards ρ_{CSLAM}; unstable?
- switch to flux-form version of CSLAM (Harris et al., 2010) and use well-known finite-volume method for coupling: SE provides accumulated background flux of air mass and CSLAM provides average flux of q (satisfies all constraints!):

$$\text{Tracer mass flux } =< q >_{CSLAM} \sum_{j=1}^{nsplit} \rho_{SE}^{(n+j/nsplit)}$$

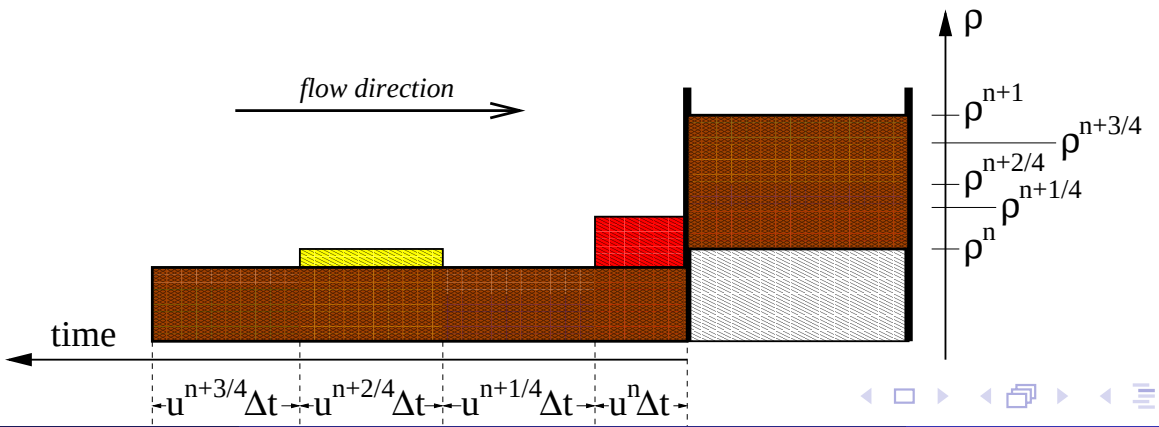

Finite-volume approach: Integrate in space

semi-Lagrangian form

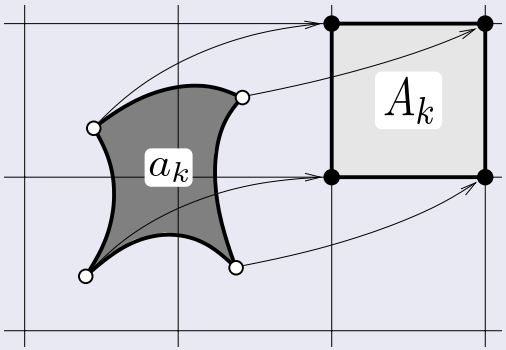

$$\frac{D}{Dt}\int_{A(t)} \psi \, dA = 0.$$

where $A(t)$ is a Lagrangian† control volume and

$$\frac{D}{Dt} = \frac{\partial}{\partial t} + \vec{v}\cdot\nabla,$$

is the material/total derivative.

Eulerian (flux-form) form

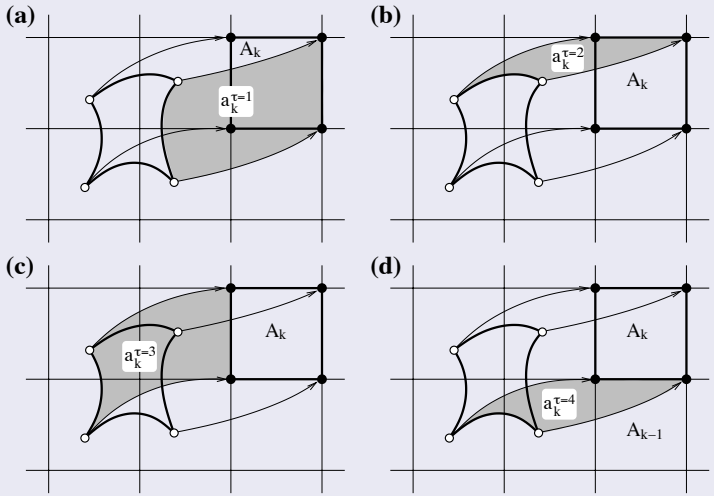

Integrate

$$\frac{\partial \psi}{\partial t} + \nabla\cdot(\psi\,\vec{v}) = 0$$

over an Eulerian control volume A_k:

$$\frac{\partial}{\partial t}\int_{A_k} \psi \, dA + \int_{A_k} \nabla\cdot(\psi\,\vec{v})\; dA = 0.$$

† volume whose bounding surface moves with the local fluid velocity $\Leftrightarrow$ volume which always contains the same material particles

Finite-volume approach: Integrate in space

semi-Lagrangian form

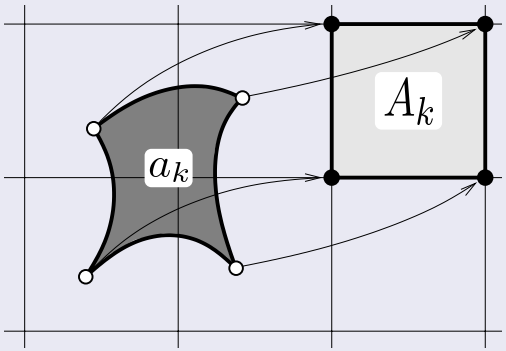

$$\frac{D}{Dt}\int_{A(t)} \psi \, dA = 0.$$

where $A(t)$ is a Lagrangian† control volume and

$$\frac{D}{Dt} = \frac{\partial}{\partial t} + \vec{v}\cdot\nabla,$$

is the material/total derivative.

Eulerian (flux-form) form

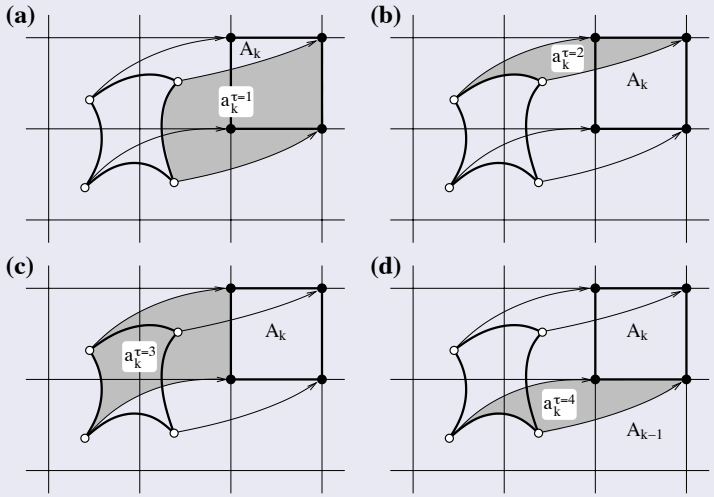

Apply divergence theorem on second term:

$$\frac{\partial}{\partial t}\int_{A_k} \psi \, dA + \oint_{\partial A_k} (\psi\,\vec{v})\cdot\vec{n}\, dS = 0,$$

where ∂A_k is the boundary of A_k and $\vec{n}$ the outward normal vector to ∂A_k.
→ instantaneous flux of tracer mass through boundaries of A_k

† volume whose bounding surface moves with the local fluid velocity ⇔ volume which always contains the same material particles

Finite-volume approach: Integrate in time

semi-Lagrangian form

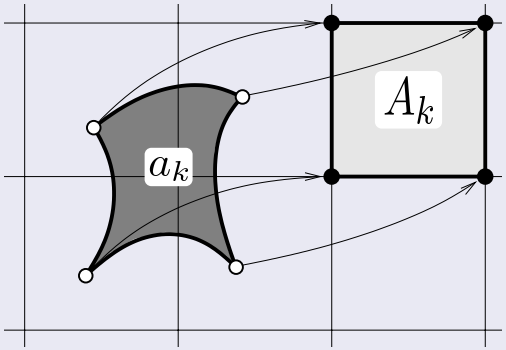

$$\int_{A(t+\Delta t)} \psi \, dA = \int_{A(t)} \psi \, dA,$$

where Δt is time-step and $t = n\,\Delta t$.

Upstream semi-Lagrangian approach:

$$\overline{\psi}_k^{n+1} \Delta A_k = \overline{\psi}_k^{n} \Delta a_k,$$

where $\overline{()}$ is average value over cell.

Eulerian (flux-form) form

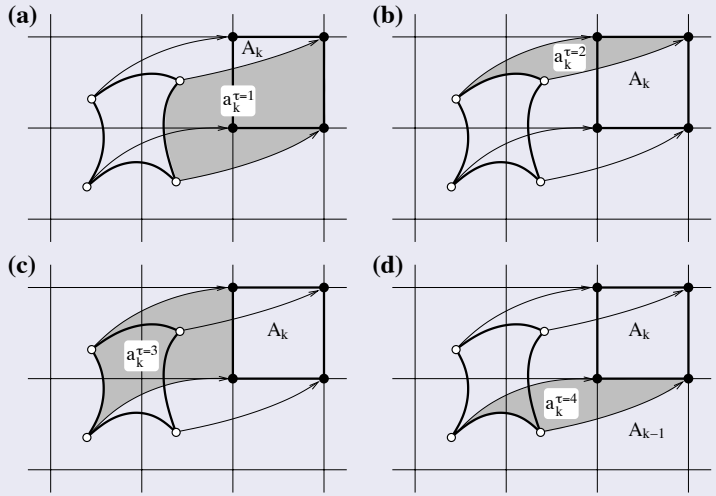

Apply divergence theorem on second term:

$$\frac{\partial}{\partial t} \int_{A_k} \psi \, dA + \oint_{\partial A_k} (\psi \, \vec{v}) \cdot \vec{n} \, dS = 0,$$

where ∂A_k is the boundary of A_k and $\vec{n}$ the outward normal vector to ∂A_k.
$\rightarrow$ instantaneous flux of tracer mass through boundaries of A_k

Finite-volume approach: Integrate in time

semi-Lagrangian form

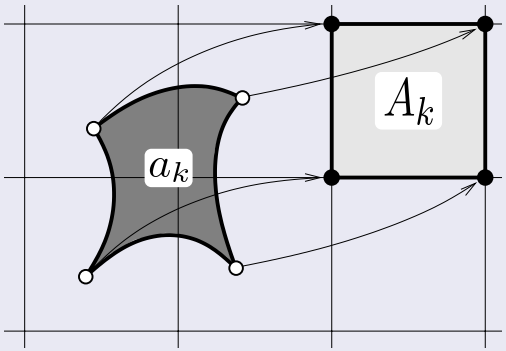

$$\int_{A(t+\Delta t)} \psi \, dA = \int_{A(t)} \psi \, dA,$$

where Δt is time-step and $t = n\,\Delta t$.

Upstream semi-Lagrangian approach:

$$\overline{\psi}_k^{n+1} \Delta A_k = \overline{\psi}_k^{n} \Delta a_k,$$

where $\overline{()}$ is average value over cell.

Eulerian (flux-form) form

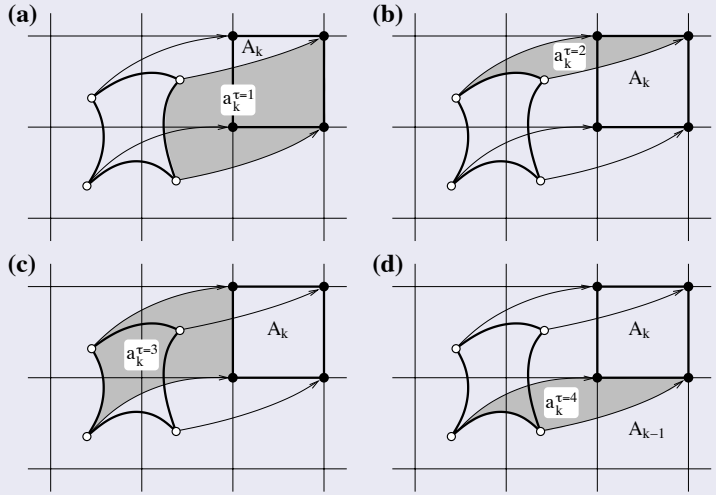

$$\frac{\partial}{\partial t} \int_{A_k} \psi \, dA + \oint_{\partial A_k} (\psi \, \vec{v}) \cdot \vec{n} \, dS = 0,$$

$$\overline{\psi}^{n+1} \Delta A_k = \overline{\psi}^{n} \Delta A_k +$$

$$\int_{n\Delta t}^{(n+1)\Delta t} \left[\oint_{\partial A_k} (\psi \, \vec{v}) \cdot \vec{n} \, dS \right] dt = 0,$$

$\rightarrow$ flux of tracer mass through boundaries of A_k during $t \in [n\Delta t, (n+1)\Delta t]$

Finite-volume approach:

semi-Lagrangian form

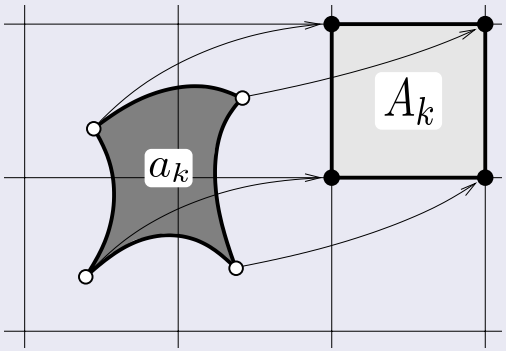

$$\int_{A(t+\Delta t)} \psi \, dA = \int_{A(t)} \psi \, dA,$$

where Δt is time-step and $t = n \, \Delta t$.

Upstream semi-Lagrangian approach:

$$\overline{\psi}_k^{n+1} \Delta A_k = \overline{\psi}_k^n \Delta a_k,$$

where $\overline{()}$ is average value over cell.

Eulerian (flux-form) form

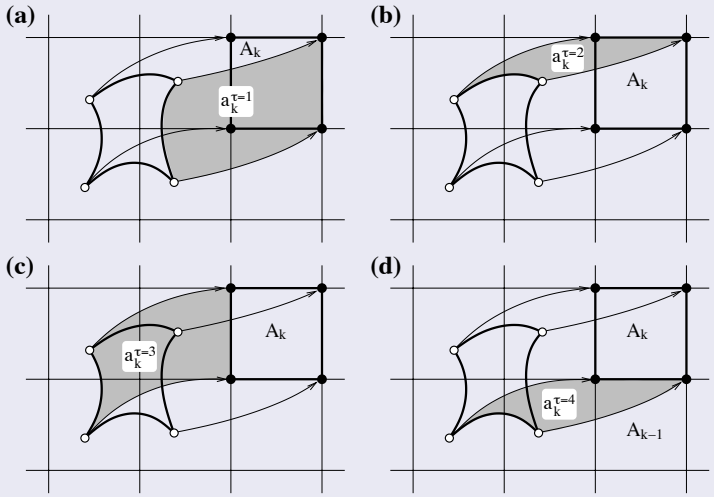

$$\overline{\psi}_k^{n+1} \, \Delta A_k = \overline{\psi}_k^n \, \Delta A_k - \sum_{\tau=1}^{4} F_k^{(\tau)},$$

where

$$F_k^{(\tau)} = s_k^{(\tau)} \int_{a_k^\tau} \psi^n(x, y) \, dA.$$

is flux of mass through face τ during Δt, and $s_k^{(\tau)} = \pm 1$

for simplicity assume s_k^τ is NOT multi-valued; for multi-valued case see, e.g., Harris et al. (2010).

Finite-volume approach:

semi-Lagrangian form

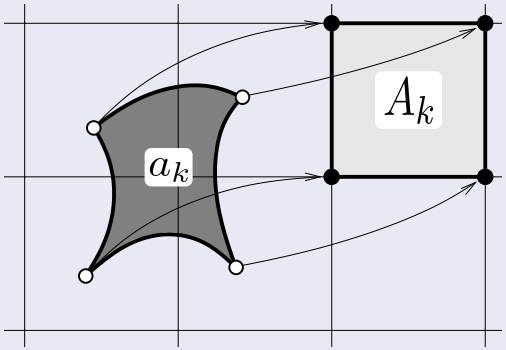

$$\overline{\psi}_k^{n+1} \Delta A_k = \overline{\psi}_k^n \Delta a_k,$$

Eulerian (flux-form) form

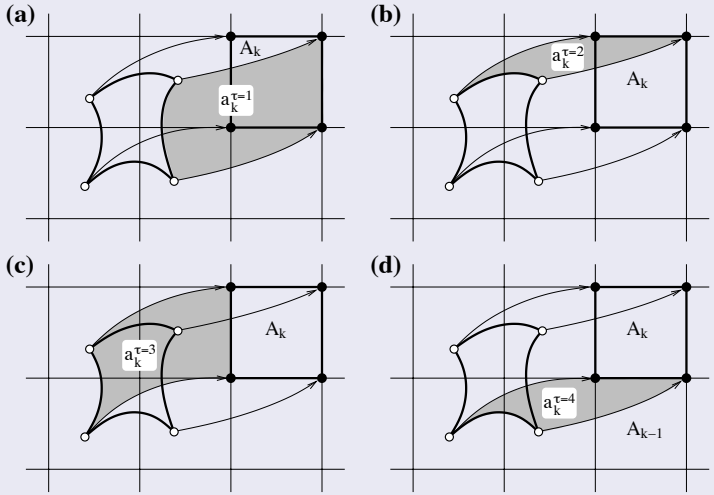

$$\overline{\psi}_k^{n+1} \Delta A_k = \overline{\psi}_k^n \Delta A_k - \sum_{\tau=1}^{4} F_k^{(\tau)},$$

Note equivalence between Lagrangian cell-integrated and Eulerian flux-form continuity equations:

$$\Delta A_k - \sum_{\tau=1}^{4} \left(s_k^{(\tau)} \Delta a_k^{(\tau)} \right) = \Delta a_k.$$

i.e. the areas involved in Eulerian forecast equals upstream Lagrangian area a_k.

Finite-volume approach:

semi-Lagrangian form

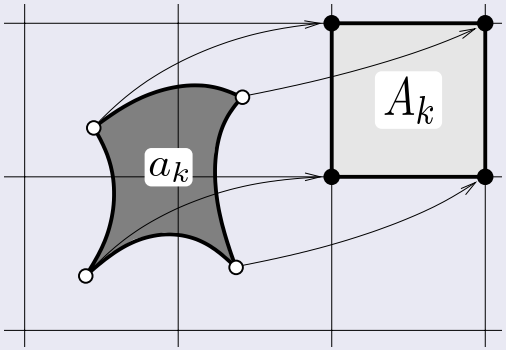

$$\overline{\psi}_k^{n+1} \Delta A_k = \overline{\psi}_k^n \Delta a_k,$$

Define a global piecewise continuous reconstruction function

$$\psi(x,y) = \sum_{k=1}^{N} I_{A_k} \psi_k(x,y),$$

where I_{A_k} is the indicator function

$$I_{A_k} = \begin{cases} 1, \ (x,y) \in A_k, \\ \\ 0, \ (x,y) \notin A_k. \end{cases}$$

Eulerian (flux-form) form

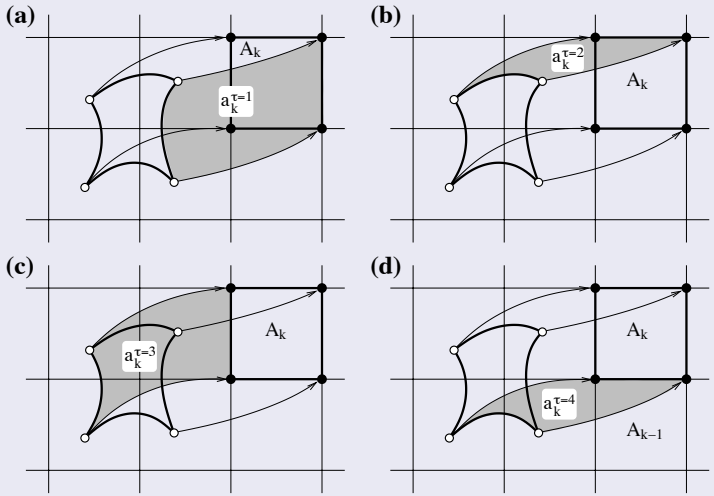

$$\overline{\psi}_k^{n+1} \Delta A_k = \overline{\psi}_k^n \Delta A_k - \sum_{\tau=1}^{4} F_k^{(\tau)},$$

Finite-volume approach:

semi-Lagrangian form

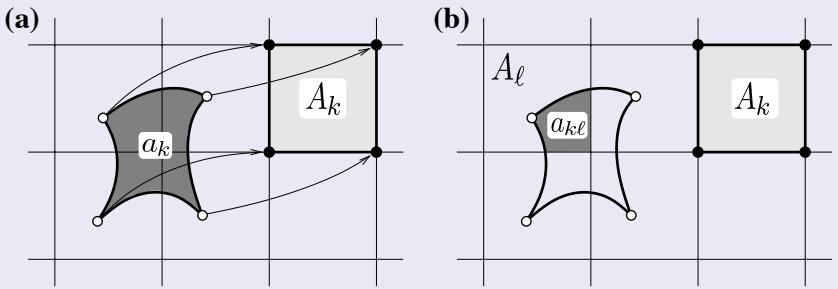

$$\overline{\psi}_k^{n+1} \Delta A_k = \overline{\psi}_k^n \Delta a_k,$$

$$\overline{\psi}_k^{n+1} \Delta A_k = \sum_{\ell=1}^{L_k} \int_{a_{k\ell}} \psi_\ell^n(x,y)\, dA.$$

where $a_{k\ell}$ is the non-empty overlap area

$$a_{k\ell} = a_k \cap A_\ell, \quad a_{k\ell} \neq \emptyset; \quad \ell = 1, \ldots, L_k,$$

where N is the number of cells in the domain and L_k number of overlap areas.

Eulerian (flux-form) form

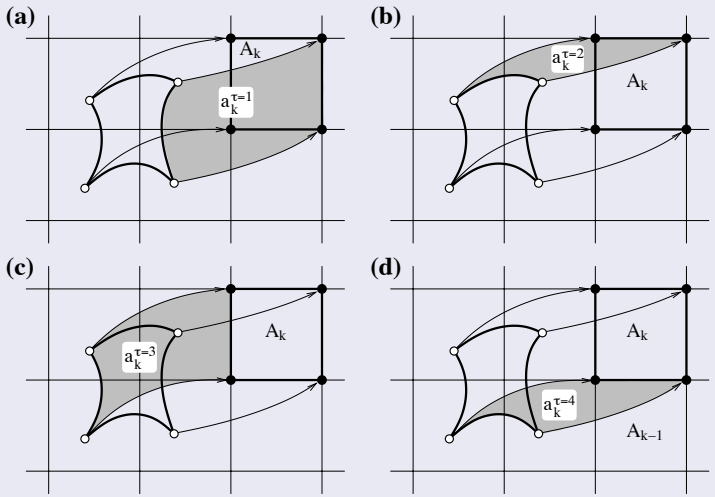

$$\overline{\psi}_k^{n+1} \Delta A_k = \overline{\psi}_k^n \Delta A_k - \sum_{\tau=1}^{4} F_k^{(\tau)},$$

Finite-volume approach:

semi-Lagrangian form

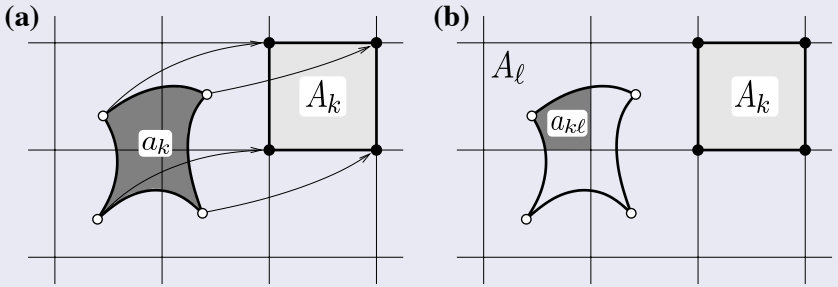

$$\overline{\psi}_k^{n+1} \Delta A_k = \overline{\psi}_k^n \Delta a_k,$$

$$\overline{\psi}_k^{n+1} \Delta A_k = \sum_{\ell=1}^{L_k} \int_{a_{k\ell}} \psi_\ell^n(x,y)\, dA.$$

where $a_{k\ell}$ is the non-empty overlap area

$$a_{k\ell} = a_k \cap A_\ell, \quad a_{k\ell} \neq \emptyset; \quad \ell = 1, \ldots, L_k,$$

where N is the number of cells in the domain and L_k number of overlap areas.

Eulerian (flux-form) form

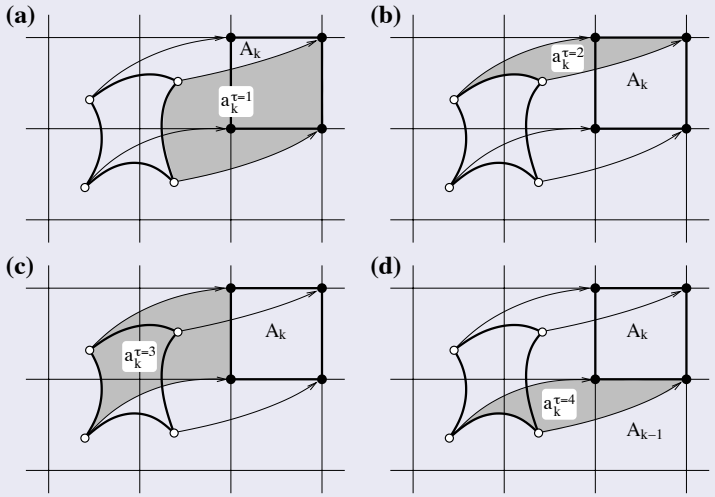

$$\overline{\psi}_k^{n+1} \Delta A_k = \overline{\psi}_k^n \Delta A_k - \sum_{\tau=1}^{4} F_k^{(\tau)},$$

$$F_k^{(\tau)} = \sum_{\ell=1}^{L_k^{(\tau)}} \int_{a_{k\ell}} \psi_\ell^n(x,y)\, dA,$$

where L_k^τ is number of non-empty 'flux' overlap areas for face τ.

Note that in general: $L_k \ll \sum_{\tau=1}^{4} L_k^{(\tau)}$

Finite-volume approach: Conditions for inherent mass-conservation

semi-Lagrangian form

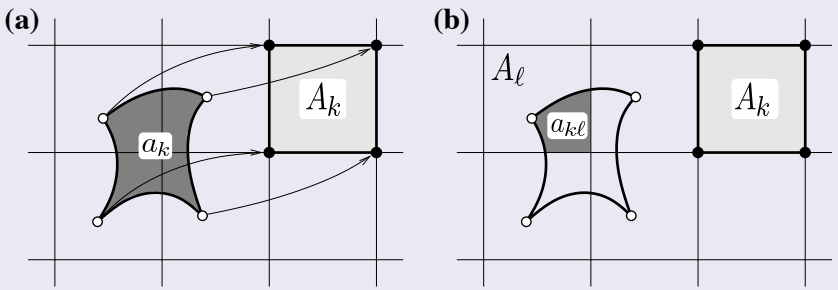

$$\overline{\psi}_k^{n+1} \Delta A_k = \overline{\psi}_k^n \Delta a_k,$$

- a_k's span Ω without gaps/overlaps

$$\bigcup_{k=1}^{N} a_k = \Omega, \text{ and } a_k \cap a_\ell = \emptyset \; \forall \; k \neq \ell.$$

- Sub-grid-scale representation of ψ must integrate to cell-average mass

$$\int_{A_k} \psi_k^n(x,y)\, dA = \overline{\psi}_k^n \Delta A,$$

Eulerian (flux-form) form

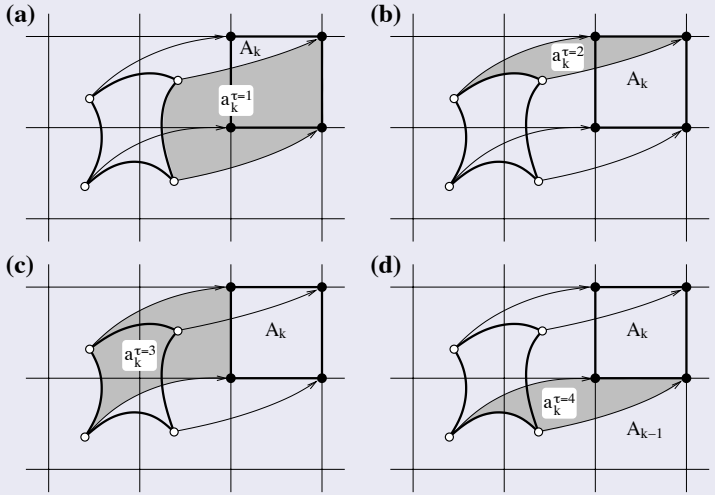

$$\overline{\psi}_k^{n+1} \Delta A_k = \overline{\psi}_k^n \Delta A_k - \sum_{\tau=1}^{4} F_k^{(\tau)},$$

- Fluxes for 'shared' faces must cancel, e.g.,

$$F_k^{(3)} = -F_{k-1}^{(1)}$$

Any flux, even highly inaccurate fluxes, will NOT violate mass-conservation!

Finite-volume approach: Enforcing shape-preservation

semi-Lagrangian form

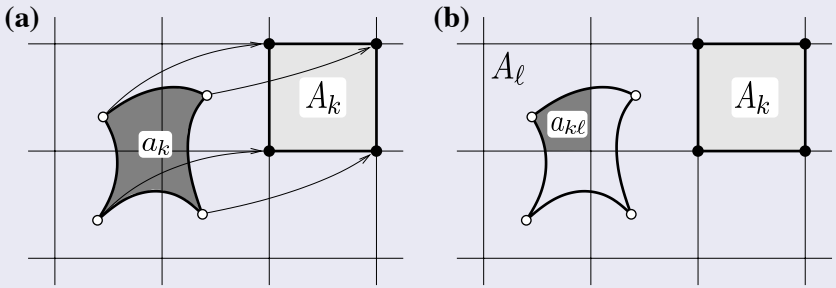

$$\overline{\psi}_k^{n+1} \Delta A_k = \overline{\psi}_k^n \Delta a_k,$$

The *only* direct way of enforcing shape-preservation is to filter the sub-grid-scale distribution $\psi_k^n(x, y)$:

- fully 2D filters (Barth and Jespersen, 1989)
- 1D filters for cascade schemes (Colella and Woodward, 1984; Zerroukat et al., 2005; Lin and Rood, 1996)

Eulerian (flux-form) form

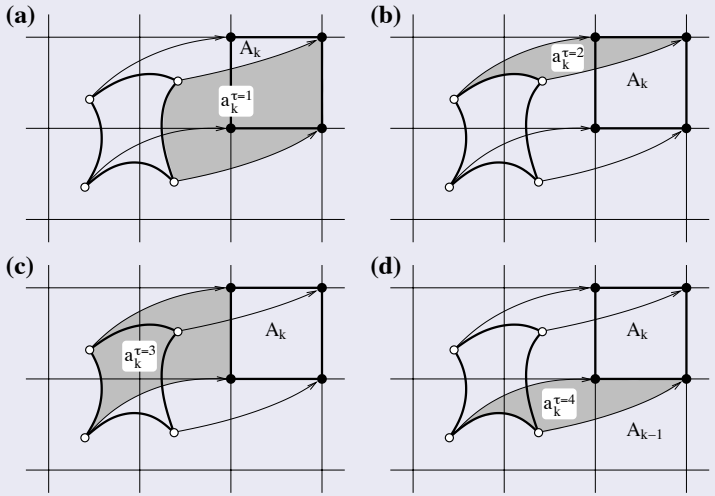

$$\overline{\psi}_k^{n+1} \Delta A_k = \overline{\psi}_k^n \Delta A_k - \sum_{\tau=1}^{4} F_k^{(\tau)},$$

Shape-preservation can be enforced by

- blending monotone and high-order fluxes (e.g., Flux-Corrected Transport Zalesak, 1979)
- making $\psi_k^n(x, y)$ shape-preserving (Barth and Jespersen, 1989)

Part II
Beyond linear transport: shallow-water model

Equations of motion

- Shallow water equations on an f-plane:

$$\begin{aligned}
\frac{\partial u}{\partial t} + u\frac{\partial u}{\partial x} + v\frac{\partial u}{\partial x} - f\,v - g\frac{\partial h}{\partial x} &= 0 \\
\frac{\partial v}{\partial t} + u\frac{\partial v}{\partial x} + v\frac{\partial v}{\partial x} + f\,u - g\frac{\partial h}{\partial y} &= 0 \\
\frac{\partial h}{\partial t} + \nabla\cdot(h\vec{v}) &= 0 \\
\frac{\partial (h\,q)}{\partial t} + \nabla\cdot(h\,q\vec{v}) &= 0
\end{aligned}$$

  where f Coriolis, h height, $\vec{v} = (u, v)$ horizontal velocity vector, g gravity.

- Momentum equation solved using traditional two-time-level semi-implicit scheme.
- Continuity equations solved with cell-integrated scheme: CSLAM
  - Semi-implicit time-stepping with cell-integrated Lagrangian schemes not straight forward (consistency, divergence discretization)

Time-stepping and coupling: mass-conservative semi-implicit approach

Traditionally: semi-Lagrangian advection of ρ is combined with semi-implicit time-stepping:

$$\overline{\rho}_k^{n+1} = \left(\overline{\rho}_k^{n+1}\right)_{exp} - \frac{\Delta t}{2}\rho_{00}\left(\nabla\cdot\vec{v}_k^{n+1} - \nabla\cdot\tilde{v}_k^{n+1}\right),$$

where

- ρ_{00} a constant reference density
- $(\cdot)_{exp}$ is the explicit prediction
- $\tilde{\vec{v}}^{n+1}$ velocity extrapolated to time-level $(n+1)$

What about tracers?

- Solving continuity equation for $(\rho\, q)$ explicitly

$$\overline{\rho\, q}_k^{n+1}\Delta A_k = \overline{\rho\, q}_k^{n}\Delta a_k$$

  is NOT 'free-stream' preserving!

- Using 'traditional' semi-implicit approach for tracers

$$\overline{\rho\, q}_k^{n+1}\Delta A_k = \overline{\rho\, q}_k^{n}\Delta a_k - \frac{\Delta t}{2}(\rho\, q)_{00}\left(\nabla\cdot\vec{v}_k^{n+1} - \nabla\cdot\tilde{\vec{v}}_k^{n+1}\right).$$

  is 'free-stream' preserving but problematic (Lauritzen et al., 2008).

Time-stepping and coupling: mass-conservative semi-implicit approach

Traditionally: semi-Lagrangian advection of ρ is combined with semi-implicit time-stepping:

$$\overline{\rho}_k^{n+1} = \left(\overline{\rho}_k^{n+1}\right)_{exp} - \frac{\Delta t}{2}\left\{\nabla\cdot\left[\left(\overline{\rho}_k^{n+1}\right)_{exp}\vec{v}_k^{n+1}\right] - \nabla\cdot\left[\left(\overline{\rho}_k^{n}\right)_{exp}\tilde{v}_k^{n+1}\right]\right\}.$$

where

- ρ_{00} a constant reference density
- $(\cdot)_{exp}$ is the explicit prediction
- $\tilde{\vec{v}}^{n+1}$ velocity extrapolated to time-level $(n+1)$

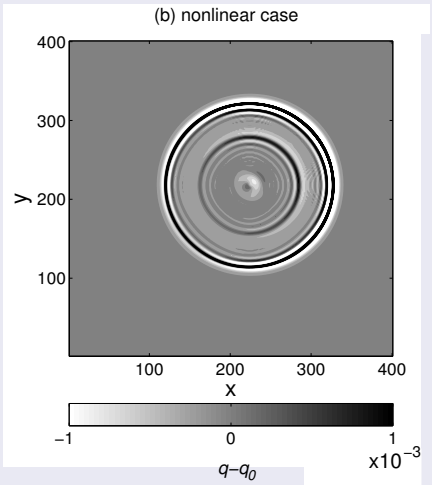

- Radially propagating gravity wave test (shallow water in Cartesian geometry; Wong et al., 2013b)
- Initial condition: $q = 1$
- Errors are $\mathcal{O}(10^{-3})$
- Problematic? Even when using a shape-preserving filter the semi-implicit correction term may render the scheme oscillatory and non-shape-preserving!

Time-stepping and coupling: mass-conservative semi-implicit approach

Traditionally: semi-Lagrangian advection of ρ is combined with semi-implicit time-stepping:

$$\overline{\rho}_k^{n+1} = \left(\overline{\rho}_k^{n+1}\right)_{exp} - \frac{\Delta t}{2}\left\{\nabla\cdot\left[\left(\overline{\rho}_k^{n+1}\right)_{exp}\vec{v}_k^{n+1}\right] - \nabla\cdot\left[\left(\overline{\rho}_k^{n}\right)_{exp}\tilde{v}_k^{n+1}\right]\right\}.$$

where

- ρ_{00} a constant reference density
- $(\cdot)_{exp}$ is the explicit prediction
- $\tilde{\vec{v}}^{n+1}$ velocity extrapolated to time-level $(n+1)$

What about tracers?

- A solution is to formulate the semi-implicit terms in flux-form

$$\overline{\rho\, q}_k^{n+1} = \left(\overline{\rho\, q}_k^{n+1}\right)_{exp} - \frac{\Delta t}{2}\left\{\nabla\cdot\left[\left(\overline{\rho\, q}_k^{n+1}\right)_{exp}\vec{v}_k^{n+1}\right] - \nabla\cdot\left[\left(\overline{\rho\, q}_k^{n}\right)_{exp}\tilde{\vec{v}}_k^{n+1}\right]\right\}.$$

  so that reference states are eliminated (Wong et al., 2013b)

Time-stepping and coupling: mass-conservative semi-implicit approach

Traditionally: semi-Lagrangian advection of ρ is combined with semi-implicit time-stepping:

$$\overline{\rho}_k^{n+1} = \left(\overline{\rho}_k^{n+1}\right)_{exp} - \frac{\Delta t}{2}\left\{\nabla\cdot\left[\left(\overline{\rho}_k^{n+1}\right)_{exp}\vec{v}_k^{n+1}\right] - \nabla\cdot\left[\left(\overline{\rho}_k^{n}\right)_{exp}\tilde{v}_k^{n+1}\right]\right\}.$$

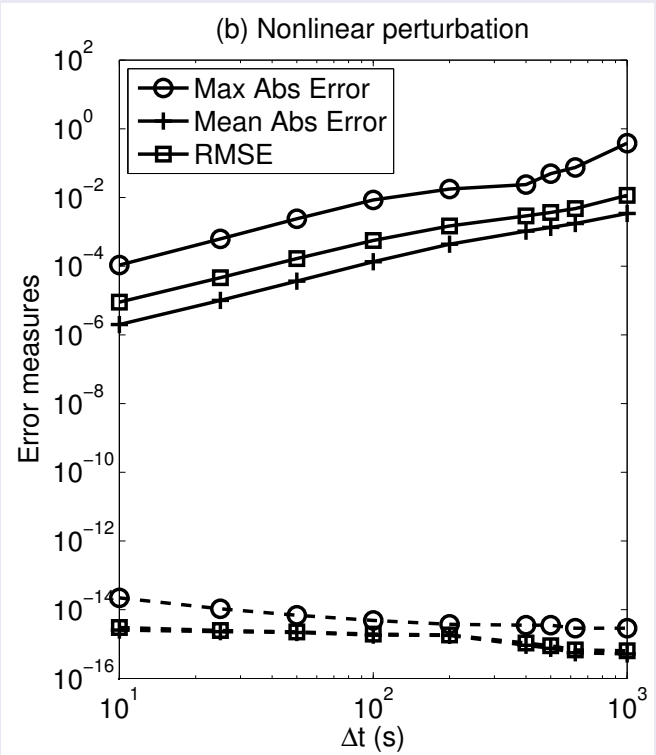

- Radially propagating gravity wave test: error measures for q as a function of Δt
  – solid lines is 'problematic' formulation
  –– dash lines is new formulation
- Initial condition: $q = 1$
- Errors in semi-implicit correction term increase with increasing Δt
- New formulation is 'free-stream preserving' and shape-preserving!
- Both formulations are stable for long Δt's

Discretization of divergence

In traditional semi-implicit semi-Lagrangian scheme, divergence is usually discretized with finite-differences:

$$\nabla_{eul} \cdot \vec{v} = \frac{u_{i+1j} - u_{ij}}{\Delta x} + \frac{v_{ij+1} - v_{ij}}{\Delta y}, \qquad (6)$$

however, cell-integrated schemes 'see' a Lagrangian discretization of divergence based on area change:

$$\nabla_{lgr} \cdot \vec{v} = \frac{1}{\Delta A_k} \frac{\Delta A_k - \delta A_k}{\Delta t} \qquad (7)$$

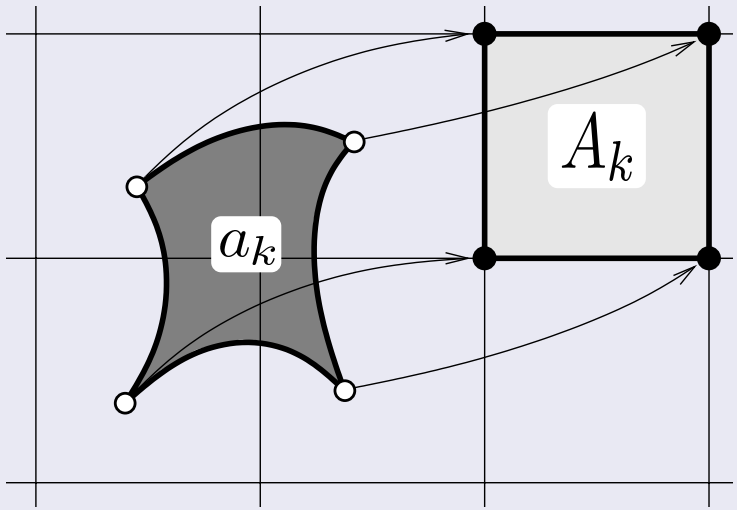

Time-stepping and coupling: mass-conservative semi-implicit approach

Simple example graphically illustrating difference between $\nabla_{eul} \cdot \vec{v}$ and $\nabla_{lgr} \cdot \vec{v}$

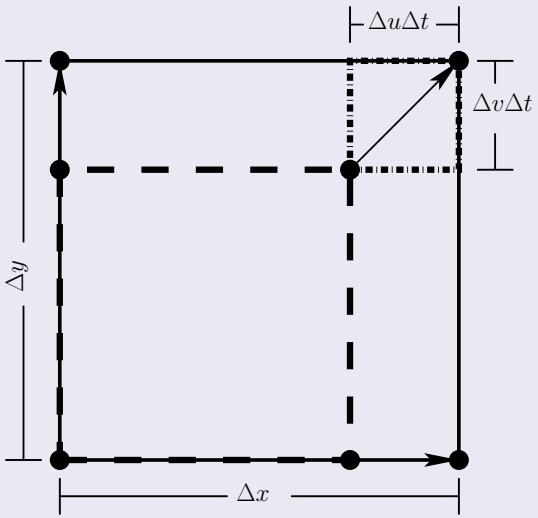

Figure: Assume the following velocity components at cell vertices

$$\begin{aligned} \vec{v}_{SW} &= (0,0), \\ \vec{v}_{NW} &= (0,v), \\ \vec{v}_{SE} &= (u,0), \\ \vec{v}_{NE} &= (u,v), \end{aligned}$$

where standard compass notation has been used.

Eulerian discretization of divergence:

$$\nabla_{eul} \cdot \vec{v} = \frac{u}{\Delta x} + \frac{v}{\Delta x} \tag{6}$$

Lagrangian (cell-integrated) discretization of divergence:

$$\nabla_{lgr} \cdot \vec{v} = \frac{u}{\Delta x} + \frac{v}{\Delta x} - \Delta t \frac{u\,v}{\Delta x\,\Delta y}. \tag{7}$$

$\rightarrow$ differ by non-linear term!

Time-stepping and coupling: mass-conservative semi-implicit approach

Simple example graphically illustrating difference between $\nabla_{eul} \cdot \vec{v}$ and $\nabla_{lgr} \cdot \vec{v}$

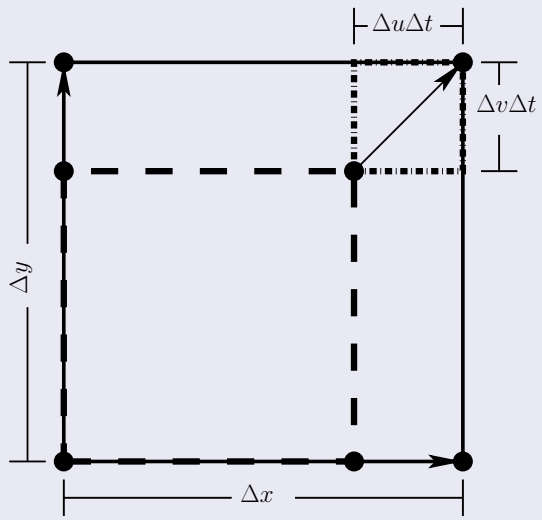

Figure: Assume the following velocity components at cell vertices

$$\begin{aligned} \vec{v}_{SW} &= (0,0), \\ \vec{v}_{NW} &= (0,v), \\ \vec{v}_{SE} &= (u,0), \\ \vec{v}_{NE} &= (u,v), \end{aligned}$$

where standard compass notation has been used.

To have consistency with CSLAM (use $\nabla_{lgr} \cdot \vec{v}$) and retain a Helmholtz equation for the semi-implicit solve, the continuity equation is discretized as follows

$$\begin{aligned} \overline{\rho\, q}_k^{n+1} = \left(\overline{\rho\, q}_k^{n+1}\right)_{exp} - \frac{\Delta t}{2}\left\{\nabla_{eul} \cdot \left[\left(\overline{\rho\, q}_k^{n+1}\right)_{exp} \vec{v}_k^{n+1}\right] - \nabla_{lgr} \cdot \left[\left(\overline{\rho\, q}_k^{n}\right)_{exp} \tilde{\vec{v}}_k^{n+1}\right]\right\} \\ + \frac{\Delta t}{2}\overline{\left\{\nabla_{eul} \cdot \left[\left(\overline{\rho\, q}_k^{n+1}\right)_{exp} \vec{v}_k^{n+1}\right] - \nabla_{lgr} \cdot \left[\left(\overline{\rho\, q}_k^{n}\right)_{exp} \tilde{\vec{v}}_k^{n+1}\right]\right\}} \frac{\delta a_k}{\Delta A_k}, \end{aligned} \quad (6)$$

(Lauritzen et al., 2006; Wong et al., 2013b)

Shallow-water channel on the plane: Gaussian jet (Poulin and Flierl, 2003)

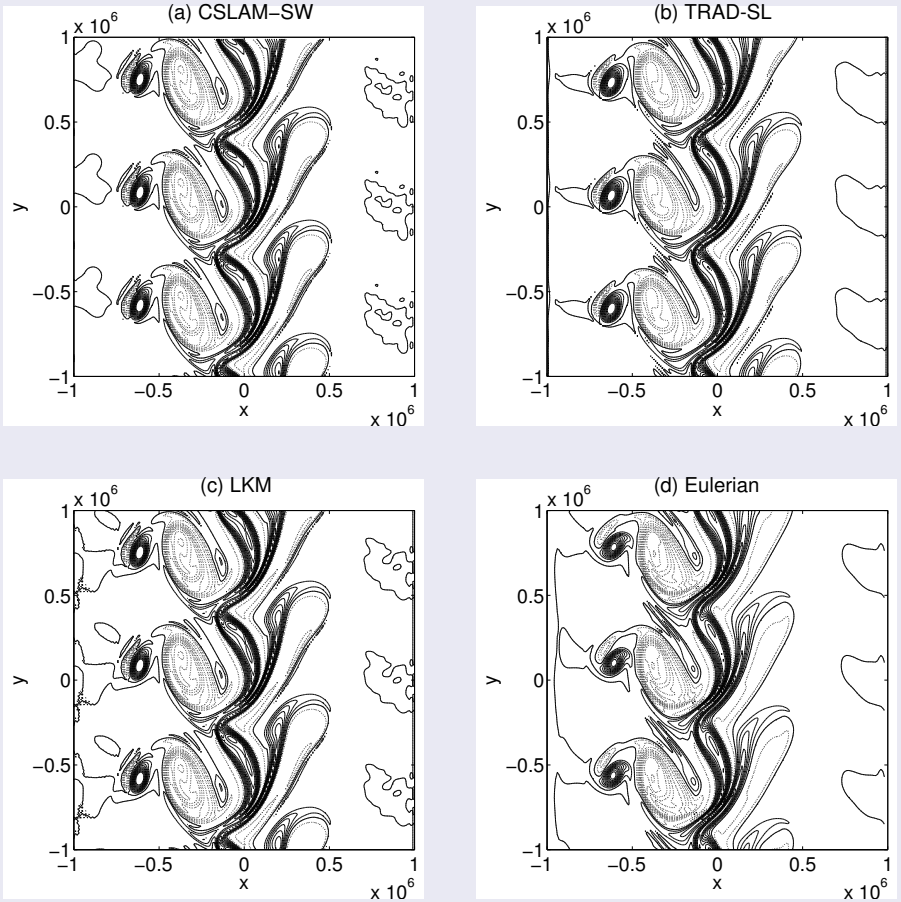

Figure: Vorticity

- (a) Traditional grid-point method for momentum equations and CSLAM for mass
- (b) Traditional grid-point method for momentum and continuity equations
- (c) Same as (a) but with 'problematic' semi-implicit method (LKM)
- (d) Eulerian discretization (semi-implicit leapfrog; Asselin filter)

Shallow-water channel on the plane: Gaussian jet (Poulin and Flierl, 2003)

(a) Non–shape–preserving CSLAM–SW

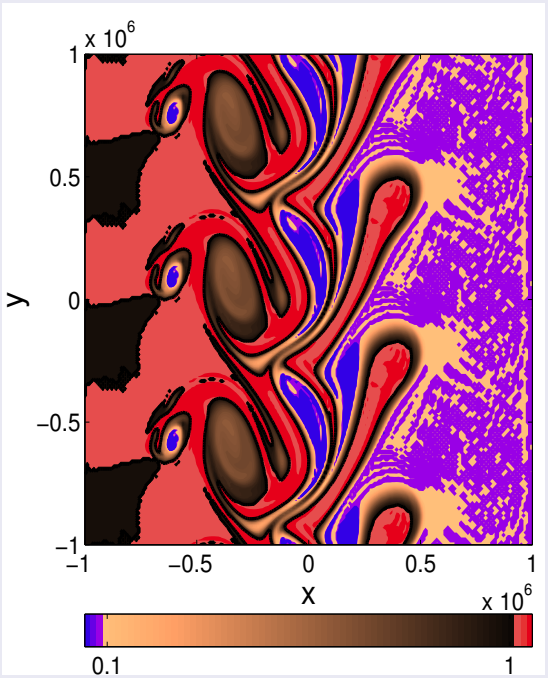

Specific concentration, q

(b) Shape–preserving LKM

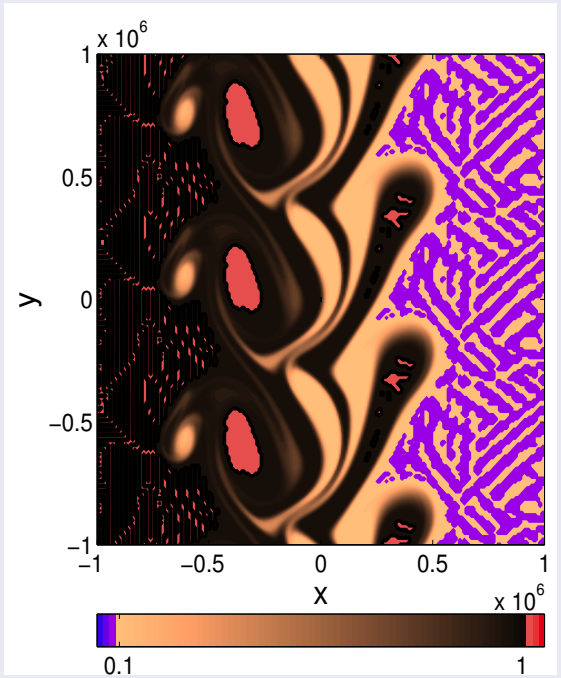

Specific concentration, q

(c) Shape–preserving CSLAM–SW

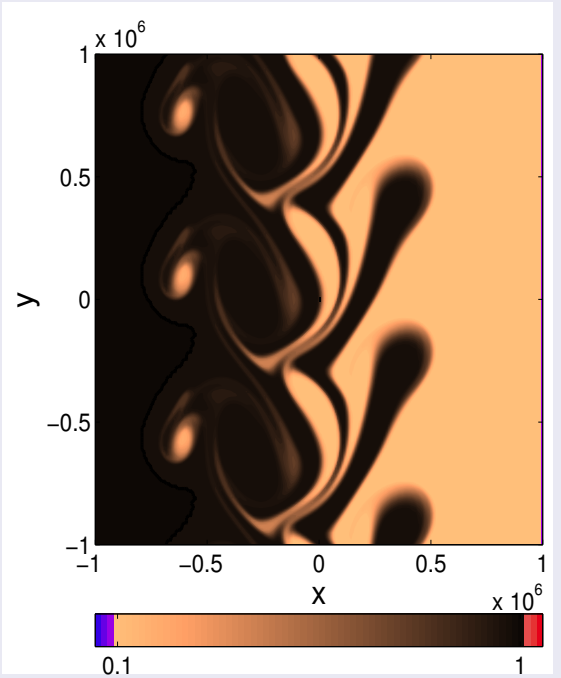

Specific concentration, q

- Note: even with shape-preserving filter on explicit advection the semi-implicit correction terms render solution non-shape-preserving for the ‘problematic formulation (LKM)

Part III
A compressible nonhydrostatic cell-integrated semi-Lagrangian semi-implicit solver (CSLAM-NH) with consistent and conservative transport

Two-dimensional $(x-z)$ moist Euler equations in Cartesian geometry

$$\frac{\partial u}{\partial t} + u\frac{\partial u}{\partial x} + w\frac{\partial u}{\partial z} = -\frac{\pi}{\rho_m}\gamma R_d \frac{\partial \Theta'_m}{\partial x} + F_u, \tag{7}$$

$$\frac{\partial w}{\partial t} + u\frac{\partial w}{\partial x} + w\frac{\partial w}{\partial z} = -\frac{\pi}{\rho_m}\gamma R_d \frac{\partial \Theta'_m}{\partial z} + \frac{g}{\rho_m}\left[\overline{\rho}_d \frac{\pi'}{\overline{\pi}} - \rho'_m\right] + F_w, \tag{8}$$

$$\frac{\partial \Theta_m}{\partial t} + \nabla \cdot (\Theta_m \mathbf{v}) = F_\Theta, \tag{9}$$

$$\frac{\partial \rho_d}{\partial t} + \nabla \cdot (\rho_d \mathbf{v}) = 0, \tag{10}$$

$$\frac{\partial Q_j}{\partial t} + \nabla \cdot (Q_j \mathbf{v}) = F_{Q_j}, \tag{11}$$

$$p = p_0 \left(\frac{R_d \Theta_m}{p_0}\right)^\gamma, \tag{12}$$

(Klemp et al., 2007)

- Equations linearized about hydrostatically balanced background state
- Momentum equations cast in their advective form
- All other equations (density, potential temperature, moist species, cast in their conservative flux-form).

Density current with mean background flow (Straka et al., 1992)

Wong et al. (2013a):

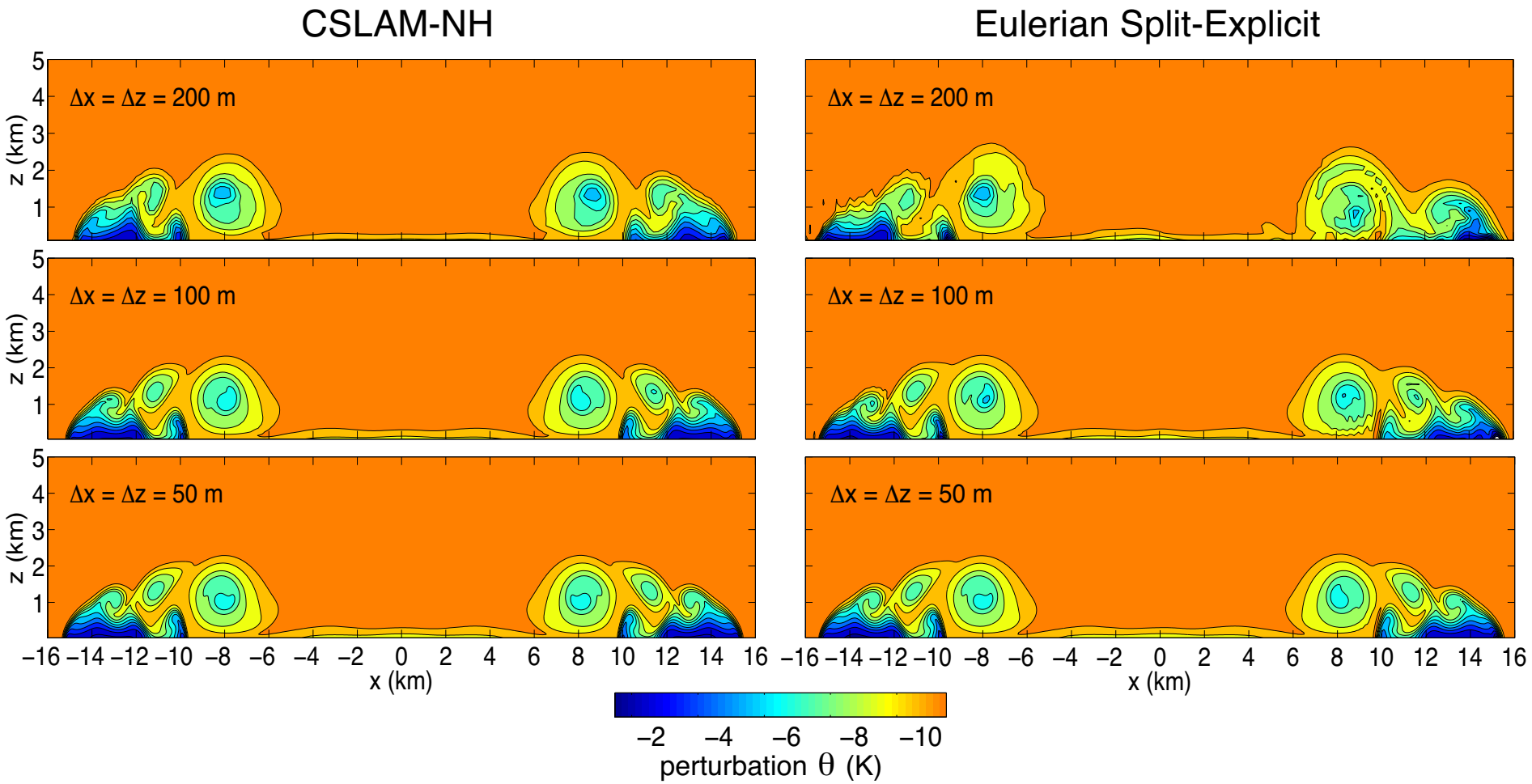

- Symmetric solutions!
- Stable with 2× split-explicit time-step

2D squall line (Weisman and Klemp, 1982)

Kessler microphysics scheme: diagnoses 'warm rain' (source/sink for water vapour, cloud water, and rainwater; latent heat release adjusts potential temperature).

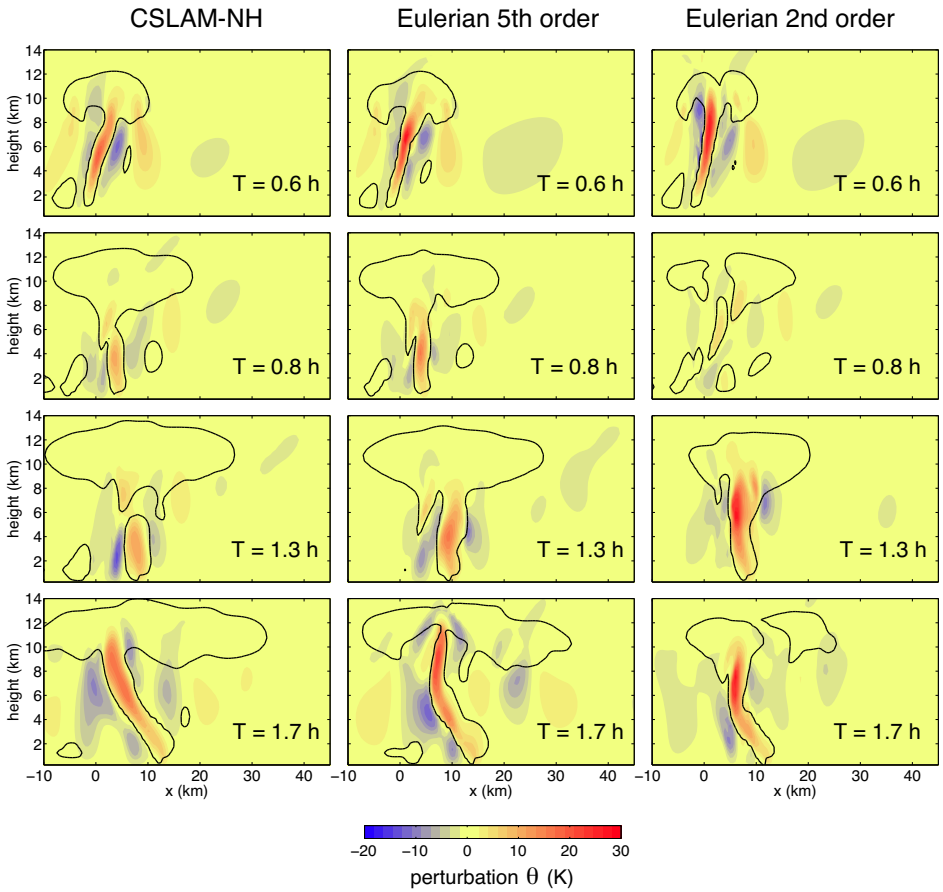

- Vertical velocity (colored contours); solid contour - convective cloud structure
- CSLAM-NH looks more like 5th-order 'WRF' solution than 2nd-order

2D squall line (Weisman and Klemp, 1982)

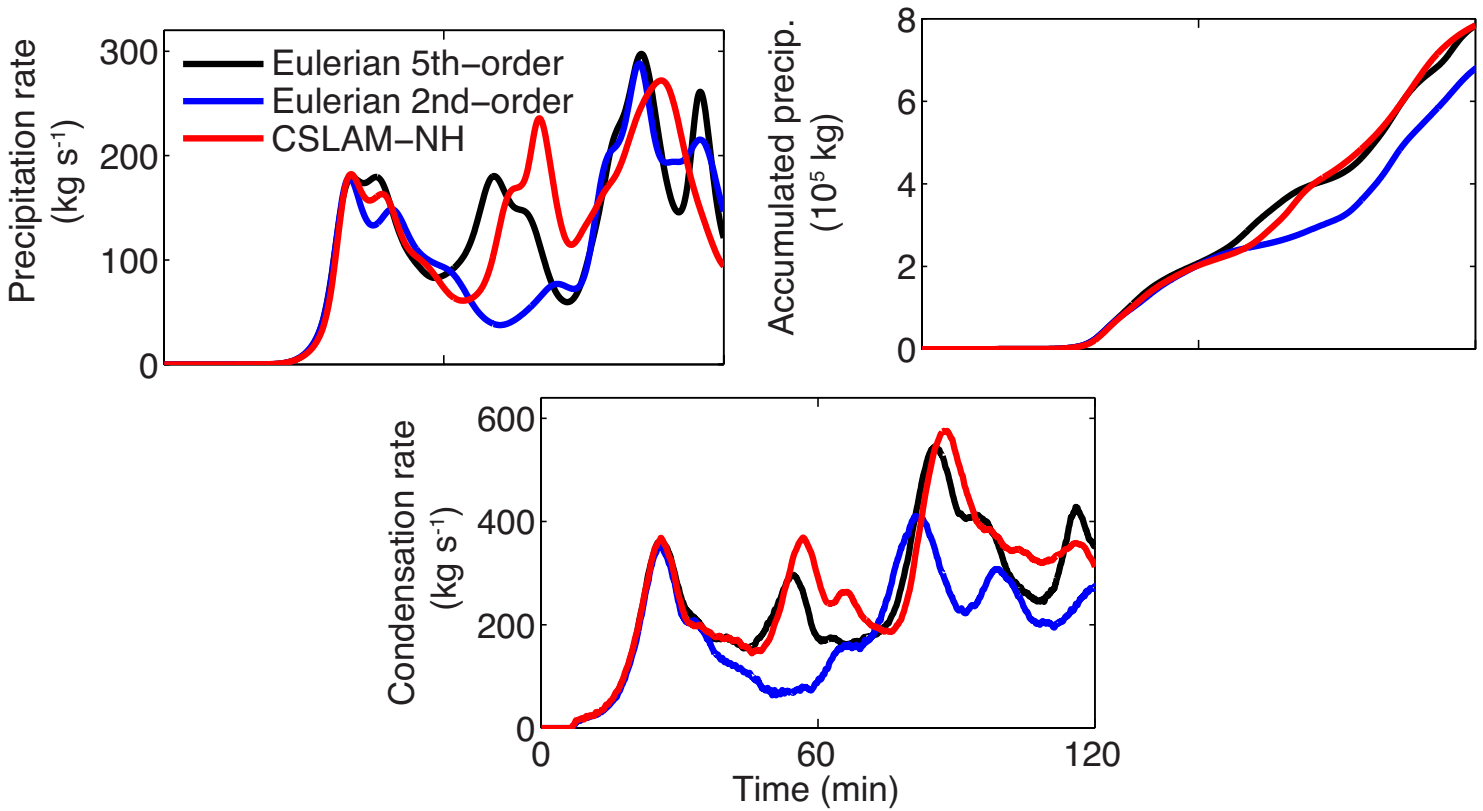

- Moisture statistics (Wong et al., 2013a)
- M. Wong is currently working on 'adding' topography to the CSLAM-NH!

Questions

References I

Barth, T. and Jespersen, D. (1989). The design and application of upwind schemes on unstructured meshes. *Proc. AIAA 27th Aerospace Sciences Meeting, Reno*.

Colella, P. and Woodward, P. R. (1984). The piecewise parabolic method (PPM) for gas-dynamical simulations. *J. Comput. Phys.*, 54:174–201.

Dennis, J. M., Edwards, J., Evans, K. J., Guba, O., Lauritzen, P. H., Mirin, A. A., St-Cyr, A., Taylor, M. A., and Worley, P. H. (2012). CAM-SE: A scalable spectral element dynamical core for the Community Atmosphere Model. *Int. J. High. Perform. C.*, 26(1):74–89.

Dukowicz, J. K. (1984). Conservative rezoning (remapping) for general quadrilateral meshes. *J. Comput. Phys.*, 54:411–424.

Dukowicz, J. K. and Baumgardner, J. R. (2000). Incremental remapping as a transport/advection algorithm. *J. Comput. Phys.*, 160:318–335.

Erath, C., Lauritzen, P. H., Garcia, J. H., and Tufo, H. M. (2012). Integrating a scalable and efficient semi-Lagrangian multi-tracer transport scheme in HOMME. *Procedia Computer Science*, 9:994–1003.

Erath, C., Lauritzen, P. H., and Tufo, H. M. (2013). On mass-conservation in high-order high-resolution rigorous remapping schemes on the sphere. *Mon. Wea. Rev.*, 141:2128–2133.

Harris, L. M., Lauritzen, P. H., and Mittal, R. (2010). A flux-form version of the conservative semi-Lagrangian multi-tracer transport scheme (CSLAM) on the cubed sphere grid. *J. Comput. Phys.*, 230(4):1215–1237.

Klemp, J., Skamarock, W. C., and Dudhia, J. (2007). Conservative split-explicit time integration methods for the compressible nonhydrostatic equations. *Mon. Wea. Rev.*, 135:2897–2913.

Lauritzen, P. and Thuburn, J. (2012). Evaluating advection/transport schemes using interrelated tracers, scatter plots and numerical mixing diagnostics. *Quart. J. Roy. Met. Soc.*, 138(665):906–918.

Lauritzen, P. H., Kaas, E., and Machenhauer, B. (2006). A mass-conservative semi-implicit semi-Lagrangian limited area shallow water model on the sphere. *Mon. Wea. Rev.*, 134:1205–1221.

Lauritzen, P. H., Kaas, E., Machenhauer, B., and Lindberg, K. (2008). A mass-conservative version of the semi-implicit semi-Lagrangian HIRLAM. *Q.J.R. Meteorol. Soc.*, 134.

Lauritzen, P. H., Nair, R. D., and Ullrich, P. A. (2010). A conservative semi-Lagrangian multi-tracer transport scheme (CSLAM) on the cubed-sphere grid. *J. Comput. Phys.*, 229:1401–1424.

Lauritzen, P. H., N.Andronova, Bosler, P. A., Calhoun, D., Enomoto, T., Dong, L., Dubey, S., Guba, O., Hansen, A., Jablonowski, C., Juang, H.-M., Kaas, E., Kent, J., Iler, R. M., J.E.Penner, Prather, M., Reinert, D., Skamarock, W., rensen, B. S., Taylor, M., Ullrich, P., and III, J. W. (2013). A standard test case suite for 2d linear transport on the sphere: results from 17 state-of-the-art schemes. *Geoscientific Model Development*. in prep.

Lauritzen, P. H., Skamarock, W. C., Prather, M. J., and Taylor, M. A. (2012). A standard test case suite for 2d linear transport on the sphere. *Geo. Geosci. Model Dev.*, 5:887–901.

References II

Lauritzen, P. H., Ullrich, P. A., and Nair, R. D. (2011). Atmospheric transport schemes: desirable properties and a semi-Lagrangian view on finite-volume discretizations, in: P.H. Lauritzen, R.D. Nair, C. Jablonowski, M. Taylor (Eds.), Numerical techniques for global atmospheric models. *Lecture Notes in Computational Science and Engineering, Springer, 2011*, 80.

Lin, S. J. and Rood, R. B. (1996). Multidimensional flux-form semi-Lagrangian transport schemes. *Mon. Wea. Rev.*, 124:2046–2070.

Margolin, L. G. and Shashkov, M. (2003). Second-order sign-preserving conservative interpolation (remapping) on general grids. *J. Comput. Phys.*, 184:266–298.

Nair, R. D. and Lauritzen, P. H. (2010). A class of deformational flow test cases for linear transport problems on the sphere. *J. Comput. Phys.*, 229:8868–8887.

Plumb, R. A. (2007). Tracer interrelationships in the stratosphere. *Rev. Geophys.*, 45(RG4005).

Poulin, F. and Flierl, G. (2003). The nonlinear evolution of barotropically unstable jets. *J. Phys. Oceanogr.*, 33:2173–2192.

Ramshaw, J. D. (1985). Conservative rezoning algorithm for generalized two-dimensional meshes. *J. Comput. Phys.*, 59(2):193–199.

Straka, J., Wilhelmson, R. B., Wicker, L. J., Anderson, J. R., and Droegemeier, K. K. (1992). Numerical solutions of a non-linear density current: A benchmark solution and comparisons. *Int. J. Numer. Methods. Fluids*, 17:1–22.

Ullrich, P. A., Lauritzen, P. H., and Jablonowski, C. (2009). Geometrically exact conservative remapping (GECoRe): Regular latitude-longitude and cubed-sphere grids. *Mon. Wea. Rev.*, 137(6):1721–1741.

Ullrich, P. A., Lauritzen, P. H., and Jablonowski, C. (2013). Some considerations for high-order 'incremental remap'-based transport schemes: edges, reconstructions and area integration. *Int. J. Numer. Meth. Fluids*, 71:1131–1151.

Weisman, M. and Klemp, J. B. (1982). The dependence of numerically simulated convective storms on vertical wind shear and buoyancy. *Mon. Wea. Rev.*, 110:504–520.

Wong, M., Skamarock, W. C., Lauritzen, P. H., Klemp, J. B., and Stull, R. B. (2013a). A compressible nonhydrostatic cell-integrated semi-lagrangian semi-implicit solver (cslam-nh) with consistent and conservative transport. *Mon. Wea. Rev.*

Wong, M., Skamarock, W. C., Lauritzen, P. H., and Stull, R. B. (2013b). A cell-integrated semi-implicit semi-Lagrangian shallow-water model (CSLAM-SW) with consistent treatment of inherently-conservative mass and scalar mass transport. *Mon. Wea. Rev.*, 141:2545–2560.

Zalesak, S. T. (1979). Fully multidimensional flux-corrected transport algorithms for fluids. *J. Comput. Phys.*, 31:335–362.

Zerroukat, M., Wood, N., and Staniforth, A. (2005). A monotonic and positive-definite filter for a semi-Lagrangian inherently conserving and efficient (SLICE) scheme. *Q. J. R. Meteorol. Soc.*, 131(611):2923–2936.